Pyrazole Urea-Based Inhibitors of p38 MAP Kinase: From Lead Compound to Clinical Candidate

John Regan,*,[†] Steffen Breitfelder,[†] Pier Cirillo,[†] Thomas Gilmore,[†] Anne G. Graham,[‡] Eugene Hickey,[†] Bernhard Klaus,[†] Jeffrey Madwed,[§] Monica Moriak,[†] Neil Moss,[†] Chris Pargellis,[‡] Sue Pav,[‡] Alfred Proto,[‡] Alan Swinamer,[†] Liang Tong,[†] and Carol Torcellini[§]

Departments of Medicinal Chemistry, Biology, and Pharmacology, Boehringer Ingelheim Pharmaceuticals, Research and Development Center, 900 Ridgebury Road, Ridgefield, Connecticut 06877

We report on a series of N-pyrazole, N′-aryl ureas and their mode of binding to p38 mitogen activated protein kinase. Importantly, a key binding domain that is distinct from the adenosine 5′-triphoshate (ATP) binding site is exposed when the conserved activation loop, consisting in part of Asp168-Phe169-Gly170, adopts a conformation permitting lipophilic and hydrogen bonding interactions between this class of inhibitors and the protein. We describe the correlation of the structure−activity relationships and crystallographic structures of these inhibitors with p38. In addition, we incorporated another binding pharmacophore that forms a hydrogen bond at the ATP binding site. This modification affords significant improvements in binding, cellular, and in vivo potencies resulting in the selection of **45** (BIRB 796) as a clinical candidate for the treatment of inflammatory diseases.

Introduction

The proinflammatory cytokines tumor necrosis factor-α (TNF-α) and interleukin-1β (IL-1β) help regulate the body's response to infections and cellular stresses.[1] However, the pathophysiological consequences resulting from chronic and excessive production of TNF-α and IL-1β are believed to underlie the progression of many inflammatory diseases such as rheumatoid arthritis (RA),[2] Crohn's disease, inflammatory bowel disease, and psoriasis.[3] Recent data from clinical trials have secured the continued use of the soluble TNF-α receptor fusion protein, etanercept, or the chimeric TNF-α antibody, infliximab, in the treatment of RA[4−8] and Crohn's disease.[9,10] The signal transduction pathway leading to the production of TNF-α from stimulated inflammatory cells, while not fully understood, has been shown to be, in part, regulated by p38 mitogen activated protein (MAP) kinase.[11] p38 MAP kinase belongs to a group of serine/threonine kinases that includes c-Jun NH2-terminal kinase (JNK) and extracellular-regulated protein kinase (ERK).[12] Upon extracellular stimulation by a variety of conditions and agents,[13] p38 is activated through bis-phosphorylation on a Thr-Gly-Tyr motif located in the activation loop. Activation is achieved by dual-specificity serine/threonine MAPK kinases, MKK3 and MKK6. Once activated, p38 can phosphorylate and activate other kinases or transcription factors leading to stabilized mRNA and an increase or decrease in the expression of certain target genes.[14−17]

In addition to the discovery of this important signal transduction pathway, pyridinyl imidazole **1** (SB 203580)[11] and analogues[18−22] have been identified as potent and selective inhibitors of p38 MAP kinase. Compound **1** was shown to be an effective orally active agent in several animal models of acute and chronic inflammation.[23] Recently, an analogue of **1**, compound **2** (SB 242235), inhibited endotoxin-induced ex vivo production of TNF-α and IL-1β in human clinical trials.[24] The interest in p38 as a viable target for drug intervention has escalated as a result of these early disclosures. In addition to a plethora of patent applications on imidazole-based compounds,[25−27] several journal papers have described strategies for the modification of **1**, by either the addition of other substituents to the imidazole or its replacement with different heterocycles. These endeavors have produced imidazoles **3**[28] and **4** (RPR200765A),[29] a pyrrole analogue of **1**,[30] oxazole **5**,[31] and pyrrolo[2,3-b]pyridine **6** (RWJ 68354).[32] Imidazole **7** (RWJ 67657)[33] was described to inhibit LPS-stimulated TNF-α production in human clinical trials.[34] Also, compounds with different structural features as compared to **1** have been reported as p38 inhibitors. These include, among others, **8** (VX-745)[35] and N,N-diaryl urea **8a**[36] as well as pyrazole ketone **9** (RO3201195)[37] and pyrimido[4,5-d]pyrimidinone **10**.[38] Indole amide **11** represents another group of p38 inhibitors.[39] A benzophenone class of p38 inhibitors, an example shown as **12** (EO1428), has recently been described.[40] Diamides (**13**) are disclosed as p38 inhibitors[41] (Chart 1).

Our focus in cytokine-regulated approaches to inflammatory diseases prompted us to evaluate the potential of p38 MAP kinase as a therapeutic target. Toward this
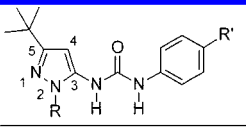
* To whom correspondence should be addressesd. Tel.: (203)798-4768.   Fax: (203)791-6072.   E-mail: jregan@rdg.boehringer-ingelheim.com.
† Department of Medicinal Chemistry.
‡ Department of Biology.
§ Department of Pharmacology.

Chart 1. Structural Classes of p38 MAP Kinase Inhibitors
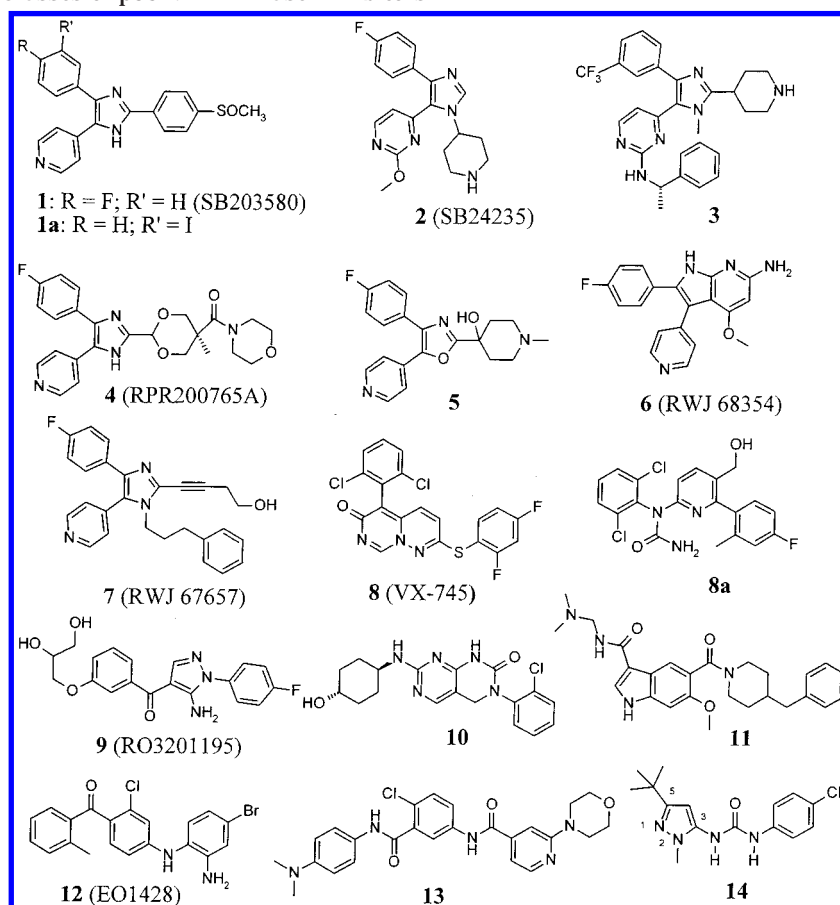
Table 1. Substitution at Pyrazole N-2

compound	R	R'	K_d (nM)	Inhibition of TNF-α in THP-1 cells EC_{50} (nM)	anal.
1	--	--	10	60	--
14	CH$_3$	Cl	350	5,900	--
16	phenyl	Cl	8	1,000	C,H,N
46	phenyl	H	13	730	C,H,N
47	cyclo-C$_6$H$_{11}$	H	500	nd^a	C,H,N
48	2-methylphenyl	H	200	2,300	C,H,N
49	3-methylphenyl	H	2	380	C,H,N
50	4-methylphenyl	H	3	180	C,H,N
51	3,4-dimethylphenyl	H	4	120	C,H,N
52	2-naphthyl	H	8	1,900	C,H,N
53	3-NH$_2$-phenyl	H	25	1,300	C,H,N
54	4-NH$_2$-phenyl	H	7	630	C,H,N
55	3-methoxyphenyl	H	19	960	C,H,N
56	4-methoxyphenyl	H	31	1,600	C,H,N
57	4-pyridinyl	H	21	820	C,H,N

^{a} not determined

end, compound **14** was identified from high throughput screening. Reports on utilizing this compound as a lead have been disclosed.[42−44] While **14** showed only a modest binding affinity for human p38 MAP kinase ($K_d = 350$ nM) (Table 1), our interest in this molecule further increased upon obtaining a cocrystal structure with recombinant human p38. The unique binding mode of
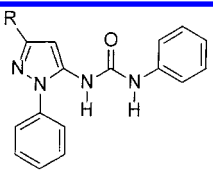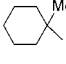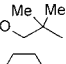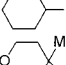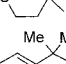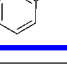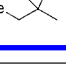
Scheme 1^a
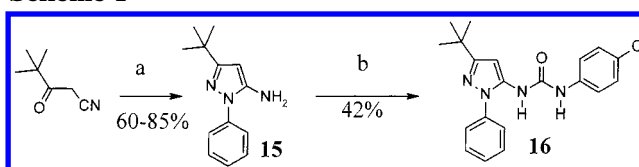
^{a} Reagents: (a) Phenylhydrazine, toluene, reflux or aqueous HCl, ethanol, reflux. (b) 4-Chlorophenyl isocyanate, THF or CH$_2$Cl$_2$, 25 °C.

14, coupled with its distinction as a new structural type of inhibitor vs others (e.g., **1**−**13**) prompted us to undertake a systematic evaluation of its pharmacophores. The structure−activity relationships (SAR) for this class of compounds and their correlation to structural data, which led to the discovery of the clinical candidate BIRB 796,[45] are the subjects of this paper.

Chemistry

Modifications to the 2-position of the pyrazole nucleus were prepared as shown in Scheme 1 using **16** as a representative example of the compounds in Table 1. The assembly of pyrazole nucleus **15** involved the condensation of phenylhydrazine and 4,4-dimethyl-3-oxopentanenitrile in either toluene or aqueous HCl in ethanol at reflux. Urea formation was accomplished with **15** and 4-chlorophenyl isocyanate to produce **16**. For examples in Table 1 requiring noncommercially available aryl hydrazines, the method of Demers[46] was used to convert aryl halides to aryl hydrazines. The cyclohexylhydrazine that was used in the synthesis of

Table 2. Substitution at Pyrazole C-5

| compound	R	K_d (nM)	anal.	compound	R	K_d (nM)	anal.
20	(cyclohexyl-Me)	22	C,H,N	61	MeO (Me Me)	1,400	C,H,N
46	*t*-butyl	13	C,H,N	62	(cyclohexyl)	>400	C,H,N
58	methyl	>7,000	C,H,N	63	(pyranyl-Me)	280	C,H,N
59	*iso*-propyl	330	C,H,N				
60	Me Me Me	12	C,H,N	64	(Me Me phenyl)	760	C,H,N

Scheme 2[a]

[a] Reagents: (a) CNCH$_2$CO$_2$H, *n*-BuLi, THF, CH$_2$Cl$_2$, −70 °C and then 25 °C. (b) Phenylhydrazine, toluene, reflux. (c) THF, 25 °C. (d) LDA, THF, MeI, −78 °C. (e) NaH, CH$_3$CN, THF, 75 °C.

target compound **47** was obtained from the sodium cyanoborohydride-mediated reductive hydrazination of cyclohexanone with hydrazine.[47]

Compound **46** was used as a frame of reference for probing the SAR at the 5-position of pyrazole by replacing the *t*-butyl moiety (Table 2). This effort required the construction of a diverse set of oxopentanenitrile subunits. Scheme 2 outlines two general procedures to prepare oxopentanenitrile derivatives. Briefly, the addition of the dianion of cyanoacetic acid[48] to acid chlorides (e.g., **17**) or the anion of acetonitrile[49] to esters (e.g., **22**) supplied the β-keto nitrile components. Following the chemistry described in Scheme 1, pyrazole formation and urea couplings were completed for target **20** as well as the other compounds in Table 2.

To evaluate the role of the urea linkage to the binding of p38, the synthesis of several urea analogues was undertaken. The biological role of each of the urea N−H groups in **16** was examined by replacement with CH$_2$ (**25** and **31**) and *N*-methyl (**34** and **37**). Amides **25** and **31** were prepared as shown in Scheme 3. EDC-mediated condensation of aminopyrazole **15** and 4-chlorophenyl-acetic acid (**24**) furnished amide **25**. Amide **31**, however, required the construction of pyrazole acetic acid **30**. Thus, pyrazolidinone **26** was converted to its O-triflate derivative **27**, which underwent Stille cross coupling with tributyl(vinyl)tin to give vinyl pyrazole **28**. Regioselective hydroboration of **28** produced alcohol **29**, which was converted to the desired carboxylic acid **30** with Jones reagent. Amide bond formation between **30** and 4-chloroaniline with DCC furnished **31**. The syntheses of *N*-methyl urea analogues **34** and **37** were undertaken as follows. Exposure of aminopyrazole **15** to phosgene[50]

Scheme 3[a]
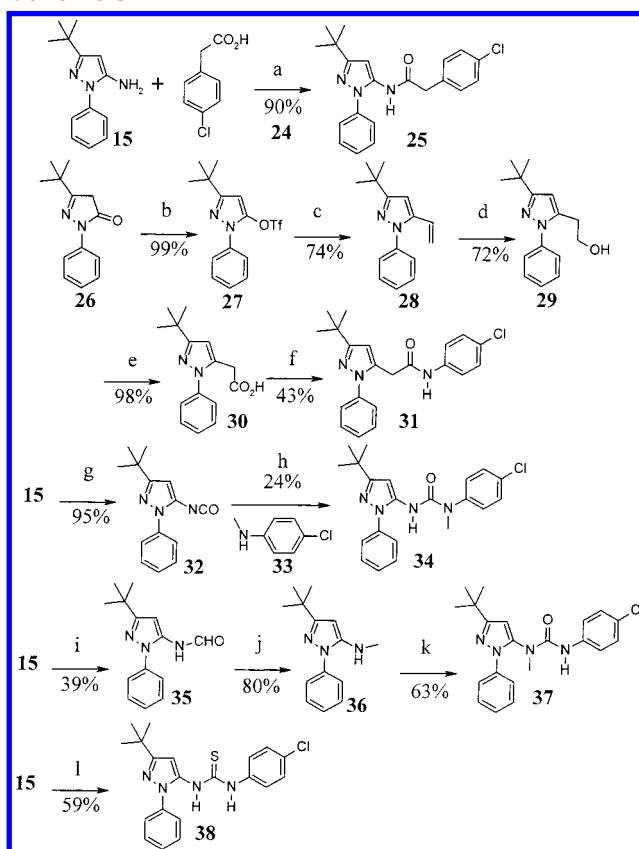
[a] Reagents: (a) EDC, CH$_2$Cl$_2$. (b) Tf$_2$O, DTBMP, CH$_2$Cl$_2$, −78 to 0 °C. (c) Tributyl(vinyl)tin, Pd[P(Ph)$_3$]$_4$, LiCl, dioxane, 100 °C. (d) (i) 9-BBN, THF, reflux. (ii) NaOH, H$_2$O$_2$. (e) Jones reagent. (f) 4-Chloroaniline, DCC, DMAP, CH$_2$Cl$_2$. (g) COCl$_2$, CH$_2$Cl$_2$, aqueous NaHCO$_3$. (h) CH$_2$Cl$_2$, 25 °C. (i) HCO$_2$H, reflux. (j) BH$_3$-DMS, THF, 25 °C. (k) 4-Chlorophenyl isocyanate, CH$_2$Cl$_2$, 25 °C. (l) 4-Chlorophenyl isothiocyanate, CH$_2$Cl$_2$, 25 °C.

produced pyrazole isocyanate **32**, which was coupled with *N*-methyl-4-chloraniline (**33**) to provide *N*-methyl urea **34**. Alternatively, aminopyrazole **15** was heated with formic acid to produce *N*-formyl aminopyrazole **35**, which upon reduction with borane[51] yielded *N*-methyl-aminopyrazole **36**. Treatment of **36** with 4-chlorophenyl isocyanate produced *N*-methyl urea analogue **37**. Thiourea **38** served as a basis to understand the part that the O-atom plays in p38 binding, and its preparation was accomplished by treatment of aminopyrazole **15** with 4-chlorophenyl isothiocyanate.

The compounds designed to explore the region of the urea phenyl of **46** are summarized in Table 4. They were conveniently obtained by the treatment of pyrazole isocyanate **32** with aniline derivatives or alkylamines. For example, as shown in Scheme 4, exposure of isocyanate **32** to 2-aminoindan (**39**) furnished urea **40**. Other target ureas were prepared according to Scheme 1 wherein amine **15** was coupled to aryl isocyanates.

To access target compounds with groups attached to the 4-position of the urea naphthalene, the route shown in Scheme 5 was utilized. Alkylation of *N*-Boc naphthol **41**, prepared from 4-amino-1-naphthol with 4-(2-chloroethyl)morpholine, gave ether **42**. Removal of the Boc protecting group (**43**) and urea formation, as described above with the isocyanate derived from **44**, gave **45**.
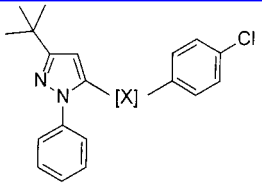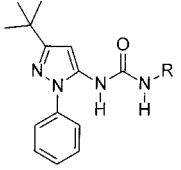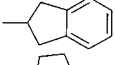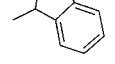
Table 3. Urea Modifications

compound	[X]	K_d (nM)	anal.
16	NHC(O)NH	8	C,H,N
25	NHC(O)CH$_2$	>900	C,H,N
31	CH$_2$C(O)NH	1,500	C,H,N
34	NHC(O)NCH$_3$	7,500	C,H,N
37	NCH$_3$C(O)NH	>1,000	C,H,N
38	NHC(S)NH	530	C,H,N

Table 4. Modification of Urea-Phenyl Ring

compound	R	K_d (nM)	Inhibition of TNF-α in THP-1 cells EC$_{50}$ (nM)	anal.
46	phenyl	13	730	C,H,N
65	H	>7,000	nd	C,H,N
66	cyclohexyl	130	3,300	C,H,N
67	2-pyridinyl	400	nd[b]	C,H,N
68	3-pyridinyl	420	nd	C,H,N
69	4-pyridinyl	1,200	nd	C,H,N
70	3-NH$_2$-phenyl	100	1,000	C,H,N
71	4-NH$_2$-phenyl	318	nd	C,H,N
72	2,3-dimethylphenyl	3	410	C,H,N
73	CH$_2$-phenyl	47	1,200	C,H,N
74	CH$_2$CH$_2$-phenyl	260	11,000	C,H,N
75	1-naphthyl	5	250	C,H,N
76	2-naphthyl	a	700	C,H,N
40		14	770	C,H,N
77		3	330	C,H,N

a. Compound's fluorescence prevents accurate measurement of K_d.
b. Not determined

Results and Discussion

We recently reported the crystal structure of recombinant human p38 MAP kinase in complex with compound **14** at 2.5 Å resolution (Figure 1).[45] Interestingly, the crystal structure reveals that this compound utilizes binding interactions on the kinase that are spatially distinct from the adenosine 5′-triphosphate (ATP) pocket. There is no structural overlap between the atoms of compound **14** and the ATP (Figure 2). Similarly, there is only limited spatial overlap between **14** and an iodo analogue of SB203580 (**1a**)[52] and this occurs in a lipophilic pocket commonly referred to in the kinase field as the specificity pocket (Figure 3). A large conformational change for conserved residues Asp168-Phe169-

Scheme 4[a]
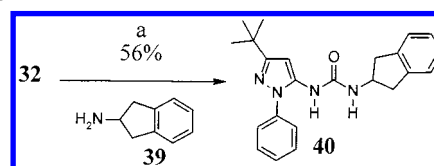
[a] Reagents: (a) CH$_2$Cl$_2$, 25 °C.

Gly170 (DFG) of the kinase is required for the observed binding mode of the diaryl urea inhibitor (Figure 2). In all of the currently known protein Ser/Thr kinase structures, the residues assume a conformation such that the Phe side chain is buried in a hydrophobic pocket in the groove between the two lobes of the kinase (DFG-in conformation). In the structure of the complex with compound **14**, however, the Phe side chain has moved by about 10 Å to a new position (DFG-out conformation). In this position, one face of the Phe side chain and the urea phenyl ring are involved in hydrophobic interactions whereas the other face is exposed to solvent. This movement of the Phe side chain reveals a large hydrophobic domain in the kinase, and the *tert*-butyl group of **14** inserts deep into this pocket (Figure 2). Neither nitrogen atom on the pyrazole ring participates in specific hydrogen-bonding interactions with the kinase. As shown in Figure 3, the urea of **14** establishes a bidentate hydrogen bond with the conserved side chain of Glu71.

Most protein kinase inhibitors use the ATP binding pocket and inhibit the kinase by directly competing with the binding of ATP. In contrast, compound **14** does not compete directly with ATP binding, as it has no structural overlap with the ATP molecule (Figure 2). However, our structure shows that the DFG-out conformation impedes ATP binding, as the side chain of the Phe residue would be sterically incompatible with the phosphate groups of ATP (Figure 2). This is supported by our observation that compound **14** interferes with the inactivation of p38 MAP kinase activity by the fluorescent ATP analogue 5′-*p*-fluorosulfonyl benzoyl adenosine (data not shown). Therefore, the diaryl urea compounds inhibit p38 MAP kinase by stabilizing a conformation of the kinase that is incompatible with ATP binding.

The data in Tables 1 and 2 highlight the binding roles of the groups appended to the pyrazole nucleus of **14**—methyl at N-2 and *tert*-butyl at C-5. Fortuitously, our first modification, replacement of the methyl of **14** with a phenyl group (**16**), improved binding potency 40-fold (Table 1) as measured in a fluorescent binding assay. The crystal structure of **16** and the recombinant human p38 complex (Figure 4) help rationalize this result. The phenyl ring at N-2 of the pyrazole participates in lipophilic interactions with the alkyl portion of the side chain of the Glu71 residue. In addition, the phenyl ring may serve as a water shield for the hydrogen bond network of the urea and the Glu71 carboxylate. The presence of the phenyl ring causes this Glu residue to adopt a side chain conformation that results in a monodentate hydrogen-bonding interaction with the urea moiety of the inhibitor. This alignment of Glu71 is in contrast to the bidentate interactions in the complex with **14** (Figure 3).

Further profiling of this key region in the inhibitor helped establish the preferred substitution at N-2 of the

Scheme 5[a]
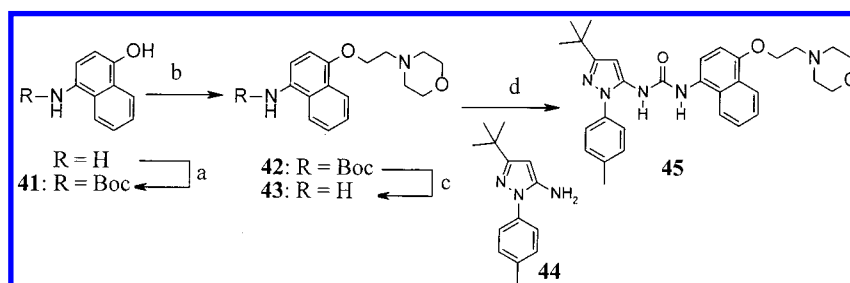
[a] Reagents: (a) Di-*tert*-butyl dicarbonate, THF, 25 °C. (b) 4-(2-Chloroethyl)morpholine, K_2CO_3, acetonitrile, heat. (c) HCl, dioxane. (d) Compound **44**, phosgene, THF.
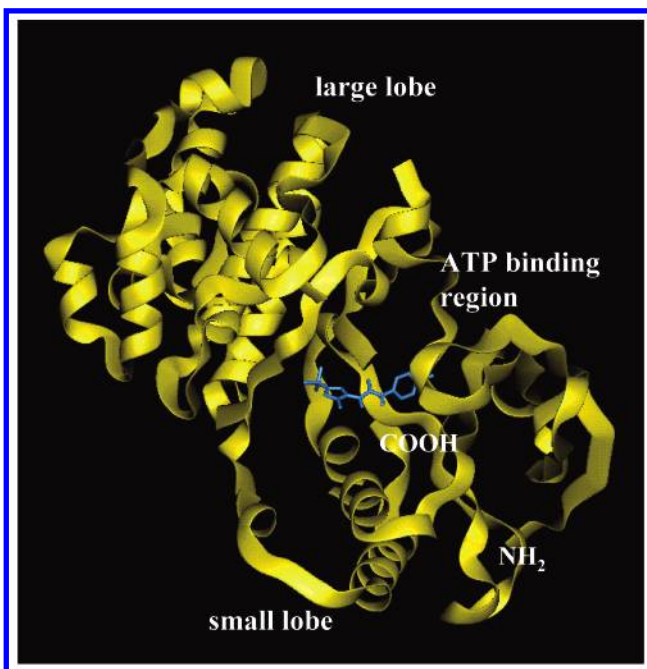

Figure 1. Crystal structure of human p38 MAP kinase and **14** at 2.5 Å resolution.

Figure 2. Overlap of **14** (blue) and ATP (red). The urea hydrogen atoms are shown for clarity. Phe169 is shown in red when occupying the DFG-in conformation (ATP bound) and in blue in the DFG-out conformation when **14** is bound to p38.

pyrazole and confirmed our hypothesis regarding binding interactions at this domain. The diminished potency of saturated derivative **47** highlighted the necessity for an aromatic ring to achieve optimal hydrophobic interactions (Table 1). Addition of methyl groups to the 3- and 4-position of the phenyl ring of **46** provided modest improvements in binding (**49**−**51**). However, 2-methyl derivative **48** displayed a substantial loss of binding affinity possibly due to an increase in the torsional angle favored between the phenyl and the pyrazole rings beyond the observed angle of 54° for **16** (Figure 4). This position tolerates bulkier groups as judged by the binding potency of 2-naphthyl analogue **52**. In addition, heteroatoms (**53**−**57**) can be accommodated at this site. The close proximity of the 3- and 4-positions of the phenyl ring of **46** to solvent may explain these results.

In Figure 4, the *tert*-butyl group at C-5 of pyrazole **16** is embedded deep into a hydrophobic pocket formed by the reorganization of Phe169 in the DFG-out conformation. In an effort to understand the binding role of the *tert*-butyl moiety in this class of compounds, we investigated the size and electronic requirements of this group. As can be seen in Table 2, removal of one methyl group lowered potency over 20-fold (cf. **46** vs **59**). Further reduction to a methyl resulted in an inactive
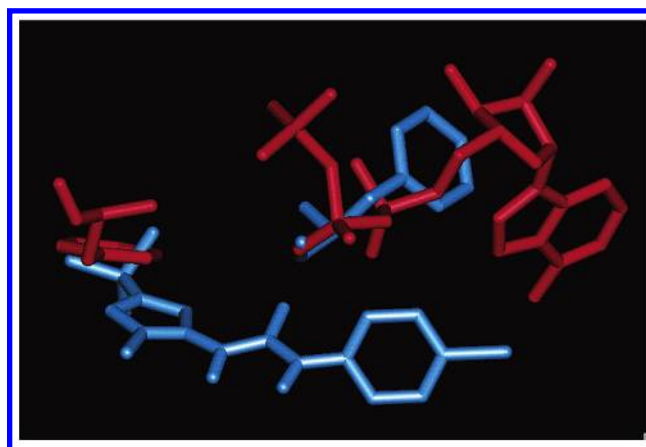
compound (**58**). This lipophilic binding pocket tolerated bulkier *tert*-alkyl groups such as dimethylethyl (**60**) and methylcyclohexyl (**20**). However, the 50-fold loss of binding observed with dimethylbenzyl analogue **64** may indicate a size limitation for this domain. A comparison of cyclohexyl derivatives **62** and **20** further exemplifies the strong preference for a tertiary group. The relatively poor activity of compounds **61** and **63** as compared to **60** and **20** suggest that lipophilic substitution at C-5 of the pyrazole is favored. Taken together, these results are rationalizable based on the crystal structure of **16** and p38 (Figure 4) that indicate a lipophilic group at C-5 of the pyrazole has important hydrophobic binding interactions with the protein in the DFG-out conformation. The *tert*-butyl group was incorporated into all subsequent target molecules since it offered the best balance of potency and physicochemical properties.

The X-ray crystallographic structure of **16** with p38 reveals a hydrogen bond network consisting of a urea hydrogen and the carboxylate oxygen of Glu71 and also the urea oxygen and N−H of Asp168. The data in Table 3 highlight the significance of these interactions on binding affinity. Replacement of either N−H in the urea with a methylene group (compounds **25** and **31**) or introduction of *N*-methyl (**34** and **37**) results in significant loss of activity. Likewise, the thiourea analogue **38** shows a 60-fold decrease in binding potency to p38 as compared to **16**. These findings underscore the crucial contribution that the urea makes to binding with p38 through extensive hydrogen bonding and, also likely, to establishing the correct geometric relationships of the other pharmacophores of the inhibitor.
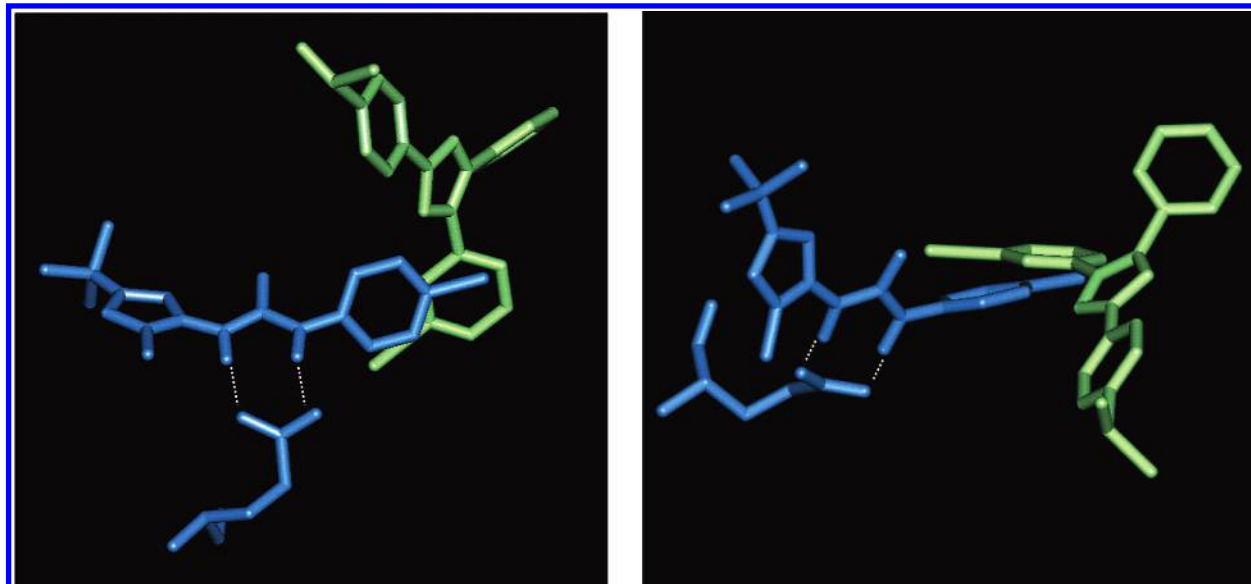
Figure 3. Two views of the overlap of **14** and **1a**. The urea hydrogen atoms are shown for clarity. The urea phenyl group of **14** occupies the same kinase specificity pocket in p38 as the phenyl ring of **1a**. The bindentate hydrogen bond interaction between the urea hydrogen atoms and the carboxylate oxygens of Glu71 is shown.
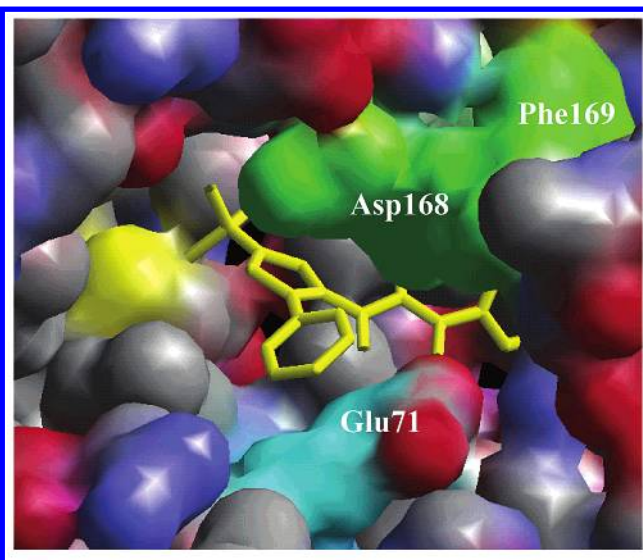

Figure 4. X-ray crystallographic structure of human p38 with **16**. The urea hydrogen atoms are shown for clarity. The hydrophobic effects of the pyrazole phenyl ring and the monodendate hydrogen bond of the urea N−H atoms with Glu71 are seen.

As seen in Figure 3, the phenyl ring attached to the urea of **14** fits into the specificity pocket of p38 in a manner similar to the pyridinyl imidazole inhibitor **1a**.[52] The importance of binding in this pocket to potency[53] and kinase specificity[28] has been described for the imidazole-based group of inhibitors. Highlights of the prominent role that the phenyl ring plays in binding with this series of compounds are shown in Table 4. Removal of the urea phenyl ring results in complete loss of binding potency (cf. **46** and **65**). Saturation of the phenyl ring (**66**) or separation of the ring from the urea by either one or two carbon atoms (**73** and **74**) resulted in decreased binding affinity. Incorporation of polar groups, through either pyridine (**67**−**69**) or aniline derivatives (**70** and **71**), lowers potency. However, lipophilic groups appended to the phenyl nucleus can improve potency (cf. **72** and **75**). Other lipophilic groups

can also provide good binding affinity as seen with bicyclic indan derivatives (**40** and **77**). Thus, these data demonstrate that the kinase specificity pocket of p38 favors lipophilic pharamacophores that are not limited to phenyl rings.

We examined several compounds from this series for oral activity in a mouse model of LPS-stimulated TNF-α synthesis. Compound **50** (Table 5) furnished an interesting and important result. The tolyl group on **50** provided a 100-fold increase in plasma concentration in the mouse vs **46**, which lacks this substitution. The increased plasma levels in combination with a modest improvement in cellular activity provided our first orally active compound. Of the 4-methylphenyl derivatives examined in this model, analogue **78** showed the best in vivo profile. This compound, with even higher plasma concentrations than **50**, suppressed TNF-α production by 90% when dosed at 100 mg/kg and also was active at 30 mg/kg (53% inhibition).

Unfortunately, we were unable to improve the in vitro and in vivo activities of the phenyl-based urea inhibitors beyond that of compound **78**. Despite available crystallographic data, obvious solutions to achieve additional binding interactions were not realized. A breakthrough arrived upon establishing a binding assay having more sensitivity for compounds whose binding activity was near the limit of the fluorescence assay.[45] One observation from this new assay suggested that **79** was more potent than initially thought. Table 6 shows selected examples of the K_d values from the fluorescence assay vs the exchange curve assay. Remarkably, naphthyl compound **79** binds 20-fold more tightly to p38 than phenyl analogue **50** despite similar cellular potencies. The overlap of the X-ray crystal structures of phenyl analogue **16** and naphthyl **75** (Figure 5) provides a possible explanation for this increased binding. The naphthyl moiety of **75** resides deep in the kinase specificity pocket and achieves substantial hydrophobic binding interactions with the protein that are not possible with the phenyl ring of **16**. Thus, it seemed reasonable that the lack of improvement in cellular

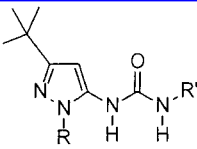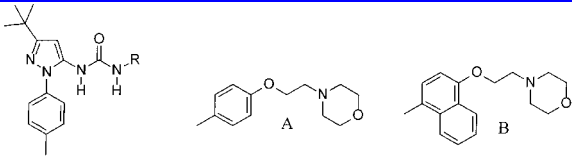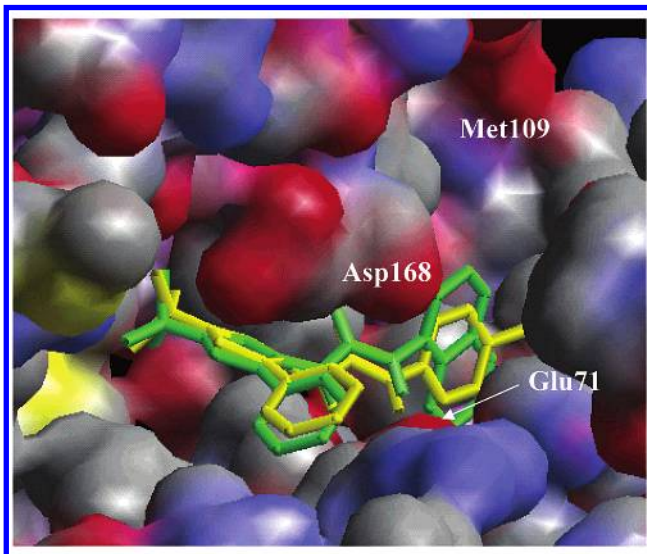**Table 5.** In Vivo Activity of Selected Pyrazole-Phenyl Ureas

compound	R	R'	K_d (nM)	Inhibition of TNF-α in THP-1 cells EC_{50} (nM)	*In Vivo* Inhibition of TNF-α at 100 mg/kg po	Mouse plasma levels at 90 minutes post dose (μg/mL)	anal.
46	phenyl	phenyl	13	730	not significant	0.1	C,H,N
50	4-methylphenyl	phenyl	3	180	67%	11	C,H,N
78	4-methylphenyl	2-fluorophenyl	14	130	90%	51	C,H,N

Table 6. Comparison of Phenyl vs Naphthyl Ureas with ATP Site Binding Pharmacophore

compound	R	Fluorescence K_d (nM)	Exchange Curve K_d (nM)	Inhibition of TNF-α in THP-1 cells EC_{50} (nM)	anal.
50	phenyl	3	21	180	C,H,N
79	1-naphthyl	1	1	370	C,H,N
80	A	88	310	6,200	C,H,N
45	B	-	0.097	18	C,H,N

Figure 5. Overlap of **16** (yellow) and **75** (green) with human p38 MAP kinase. The urea hydrogen atoms are shown for clarity. The naphthyl group of **75** fits deeper into the kinase specificity pocket as compared to the phenyl ring of **16**. The 4-position of the naphthalene ring points toward the hinge region and solvent. Phe169 is removed for clarity.

activity of **79** might be a consequence of its higher lipophilicity as compared to **50**.

The crystal structure of **75**, in addition to providing a rationale to the improved binding affinity of the naphthalene group, offered an opportunity to explore modifications from this platform that would be unavail-

able from the phenyl ring of **16**. That is, groups appended to the 4-position of the naphthalene could much more readily access the ATP binding region of p38 than the 4-positon of the phenyl ring. Hence, pharmacophores attached to the 4-position could have additional binding interactions or be used to improve physicochemical properties. The ethoxy morpholine group proved to be a very effective group for achieving both of these goals. This moiety improved binding potency 10-fold and, more significantly, increased cell activity over 20-fold. A crystal structure of **45** with recombinant human p38 (Figure 6a) provided an explanation for the enhanced potency.[45] The gauche conformation of the ethoxy linker of **45**[54,55] effectively orients the morpholine group so that the morpholine oxygen can achieve a strong hydrogen bond with the N−H of Met109. This hydrogen bond is the same one used by the adenine base of ATP and the pyridine nitrogen of the pyridinyl imidazole class of compounds such as **1a**.[52] The favorable edge to π hydrophilic interactions of the phenyl ring of Phe169 and the naphthalene group of **45** is revealed in Figure 6b and likely further contributes to binding potency.

To highlight the contribution of the naphthalene group to **45**, we prepared phenyl derivative **80**. Despite the inclusion of the ethoxy morpholine unit in phenyl analogue **80**, it exhibited a dramatic loss in potency vs **45** (Table 6). This result reinforces the importance of the naphthalene ring in providing better lipophilic interactions with the specificity pocket and properly aligning the ethoxy morpholine unit for productive binding with the ATP binding region.

In addition to superior in vitro and cellular activities, compound **45** demonstrated enhanced in vivo potency. For example, in a mouse model of LPS-stimulated TNF-α synthesis, a 65% inhibition of TNF-α synthesis was observed when **45** was dosed orally at 10 mg/kg. In a 5 week model of established collagen-induced arthritis using B10.RIII mice, **45** produced a 63% inhibition of arthritis severity when dosed orally at 30 mg/kg qd.[56] Some pharmacokinetic data of **45** in mice and cynomolgous monkeys are summarized in Table 7. The selectivity profile against a panel of protein kinases for **45** was determined and is shown in Table 8.[45] On the basis of these and other data, compound **45** (BIRB 796) was selected for human clinical trials.
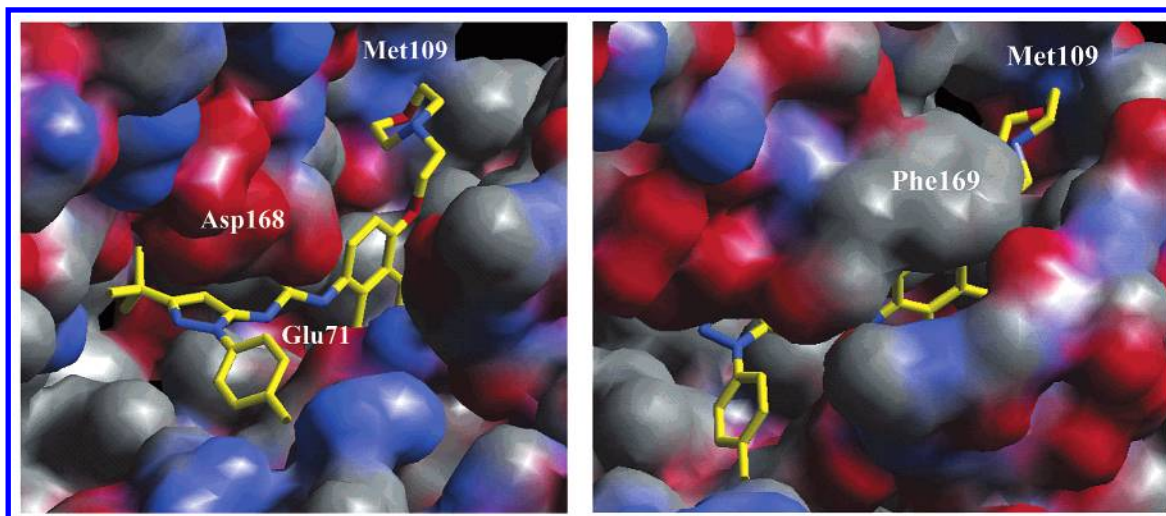
Figure 6. (a) X-ray crystallographic complex of human p38 and **45**. Phe169 is removed for clarity. (b) X-ray crystallographic complex of human p38 and **45** with Phe169.

Table 7. Pharmacokinetic Properties of Compound **45**

	Intravenous dosing at 1 mg/kg (70% PEG 400)				Oral dosing at 10 mg/kg (100% PEG 400)			
species	AUC (0-infinity) (ng*h/ml)	Vss (L/kg)	Cl (ml/min/kg)	T1/2 (hrs)	Cmax (ng/ml)	Tmax (hrs)	AUC (0-infinity) (ng*h/ml)	BA (%)
Female Balb/c mice	51,000	0.07	0.33	2.6	27,000	1.0	118,000	23
Male cynomolgous monkey	1,150	1.9	14.4	1.6	1,700	3.0	10,000	80

Table 8. Selectivity Profile of Compound **45**

Kinase	Kinase assay IC50 (μM)	Kinase	Kinase assay IC50 (μM)
Erk-1	>20	Zap70	>20
c-Raf-1	1.4	EGFR	>20
p59Fyn	>20	Her2	>20
p56Lck	>20	PKA	>20
Syk	>20	IKK2β	>20
PKCα,β,γ	>20	Jnk2α2	0.1

Conclusion

We have shown that a series of N-pyrazole, N′-aryl ureas occupy a binding domain on p38 that is exposed when the conserved binding loop, consisting in part of Asp168-Phe169-Gly170, adopts a conformation (DFG-out) not previously noted in other protein Ser/Thr kinases. A 40-fold improvement in binding was achieved by the replacement of the methyl group in the original screening lead (**14**) with phenyl. The urea atoms, shown to be involved in an extensive hydrogen bond network with Glu71 and Asp168 (Figures 3 and 4), proved critical for binding activity. A toluene ring attached to the pyrazole nucleus was necessary to secure high plasma levels in the mouse. The naphthalene was a preferred pharmacophore as compared to phenyl to bind in the kinase specificity pocket. We added an ethoxy morpholine pharmacophore, which successfully extended the binding of the inhibitor to also include a hydrogen-bonding interaction in the ATP binding region of p38. This modification afforded significant improvements in binding affinity, cellular activity, and in vivo reduction of TNF-α production and arthritis severity that resulted in the selection of **45** (BIRB 796) as a clinical candidate for the treatment of inflammatory diseases.[45,57]

Experimental Section

All solvents and reagents were obtained from commercial sources and used without further purification unless indicated otherwise. Melting points were obtained from a Mel-temp 3.0 or Fisher-Johns melting point apparatus and are uncorrected. [1]H nuclear magnetic resonance (NMR) spectrum were recorded on either a Bruker AC-F-270 spectrometer or Bruker Avance DPX 400 spectrometer. Chemical shifts are reported in parts per million (δ) from the tetramethylsilane resonance in the indicated solvent. Mass spectra were obtained from a Finnigan-SSQ7000 spectrometer. Samples were generally introduced by particle beam and ionized with NH_4Cl. Thin-layer chromatography (TLC) analytical separations were conducted with E. Merck silica gel F-254 plates of 0.25 mm thickness and were visualized with UV or I_2. Flash chromatographies were performed according to the procedure of Still et al. (EM Science Kieselgel 60, 70−230 mesh). Elemental analysis were performed at Quantitative Technologies, Inc., Whitehouse, NJ.

1-(5-*tert*-Butyl-2-phenyl-*2H*-pyrazol-3-yl)-3-(4-chlorophenyl)urea (16). A solution of phenyl hydrazine (0.83 mL, 8.39 mmol) and 4,4-dimethyl-3-oxo-pentanenitrile (1.0 g, 8.0 mmol) in toluene (3 mL) was heated to reflux overnight. Removal of the volatiles in vacuo provided a residue, which was purified by silica gel chromatography using 50% ethyl acetate in hexanes as the eluent. Concentration in vacuo of the product-rich fractions provided 3-amino-5-*tert*-butyl-2-phenyl-*2H*-pyrazole (**15**) as a light orange solid (1.53 g, 89%). A solution of **15** (0.058 g 0.27 mmol) and 4-chlorophenyl isocyanate (0.038 g, 0.25 mmol) in CH_2Cl_2 (1 mL) was stirred overnight at room temperature under inert atmosphere. Removal of the volatiles in vacuo provided a residue, which was triturated with 50% dichloromethane in hexanes (2 mL). The urea (**16**) was filtered and dried in vacuo to afford 0.078 g (85%) and was then recrystallized from methanol to afford analytically pure material; mp 202−203 °C. ^{1}H NMR (400

MHz, dimethyl sulfoxide (DMSO)-d_6): δ 1.27 (s, 9H, *tert*-butyl), 6.36 (s, 1H, pyrazole), 7.28−7.30 (m, 2H, aromatic), 7.39−7.43 (m, 3H, aromatic), 7.50−7.52 (m, 4H, aromatic), 8.42 (s, 1H, urea), 9.12 (s, 1H, urea). MS (NH$_3$-CI): *m/e* 369 (MH$^+$). Anal. (C$_{20}$H$_{21}$ClN$_4$O·CH$_3$OH) C, H, N.

1-[5-(1-Methylcyclohexyl)-2-phenyl-*2H*-pyrazol-3-yl]-3-phenyl-urea (20). A solution of cyclohexane-1-methyl-1-carboxylic acid (1.31 g, 9.21 mmol), oxalyl chloride (5.5 mL of a 2.0 M solution in CH$_2$Cl$_2$, 11.05 mmol), and a drop of anhydrous dimethylformamide (DMF) in CH$_2$Cl$_2$ (5 mL) was heated to reflux for 3 h and cooled to ambient temperature to give **17**. In a separate flask to a solution of cyanoacetic acid (1.57 g, 18.4 mmol, freshly dried with MgSO$_4$) and a catalytic amount of 2,2′-bipyridine in anhydrous tetrahydrofuran (THF) (68 mL) at −70 °C under an inert atmosphere was added dropwise *n*-butyllithium (15 mL of a 2.5 M solution in hexanes, 37.2 mmol). The mixture was slowly warmed to 0 °C until a persistent red-colored slurry was obtained. The mixture was cooled to −70 °C, and **17** in CH$_2$Cl$_2$ was slowly added. The mixture was slowly warmed to room temperature, stirred for 1 h, and quenched with 2 N aqueous HCl. The aqueous layer was extracted twice with CHCl$_3$. The combined organic layers were washed with saturated aqueous NaHCO$_3$ and brine and dried (MgSO$_4$). Removal of the volatiles in vacuo provided a residue, which was purified by silica gel chromatography using ethyl acetate in hexanes as the eluent. Concentration in vacuo of the product-rich fractions provided 1.26 g of **18**. A mixture of **18** (0.80 g, 4.8 mmol) and phenylhydrazine (0.48 mL, 4.8 mmol) in dry toluene (6 mL) was heated to reflux overnight. Removal of the volatiles in vacuo provided a residue, which was purified by silica gel chromatography. Concentration in vacuo of the product-rich fractions provided 1.10 g (90%) of **19**. A mixture of **19** (0.288 g, 1.13 mmol) and phenyl isocyanate (0.12 mL, 1.1 mmol) in anhydrous THF (4 mL) was stirred overnight under inert atmosphere. Removal of the volatiles in vacuo provided a residue, which was purified repeatedly by silica gel chromatography. Concentration in vacuo of the product-rich fractions provided 0.066 g of **20** as a foam, which softens at 86−88 °C. ^{1}H NMR (400 MHz, DMSO-d_6): δ 1.95 (s, 3H, methyl), 1.43−1.50 (m, 8H, cyclohexyl), 1.98−2.00 (m, 2H, cyclohexyl), 6.36 (s, 1H, pyrazole), 6.95−6.99 (m, 1H, aromatic), 7.24−7.30 (m, 2H, aromatic), 7.40−7.46 (m, 3H, aromatic), 7.53−7.57 (m, 4H, aromatic), 8.42 (s, 1H, urea), 9.03 (s, 1H, urea). MS (+ES): *m/e* 374 (M$^+$). Anal. (C$_{23}$H$_{26}$N$_4$O) C, H, N.

3-(4-Methyltetrahydropyran-4-yl)-3-oxo-propionitrile (23). To a solution of LDA (prepared from *n*-butyllithium (3.1 mL of a 2.5 M solution in hexanes, 7.78 mmol) and *N,N*-di-*iso*-propylamine (1.09 mL, 7.78 mmol) in THF (2 mL) at −78 °C) was added dropwise pyran **21**[58] (1.12 g, 7.78 mmol) in THF (3 mL). The mixture was stirred for 15 min, warmed to 0 °C, stirred for 30 min, and cooled to −78 °C. Methyl iodide (0.48 mL, 7.78 mmol) was added, and the mixture was stirred overnight while warming to room temperature. Ethyl acetate and aqueous HCl were added, and the organic layer was washed with brine and dried (MgSO$_4$). Removal of the volatiles in vacuo provided a residue, which was purified by silica gel chromatography using 25% ethyl acetate in hexanes as the eluent. Concentration in vacuo of the product-rich fractions provided 0.345 g (28%) of **22**. To a suspension of hexane-washed NaH (0.090 g of 60% dispersion in mineral oil, 2.2 mmol) in THF (2 mL) at 75 °C was added dropwise **22** (0.32 g, 2.03 mmol) and anhydrous acetonitrile (0.14 mL, 2.63 mmol) in THF (2 mL). The mixture was stirred for 5 h, cooled to room temperature, and diluted with ethyl acetate and aqueous HCL. The organic layer was washed with water and brine and dried (MgSO$_4$). Removal of the volatiles in vacuo provided **23** (0.244 g, 72%), which was used without further purification.

***N*-(5-*tert*-Butyl-2-phenyl-*2H*-pyrazol-3-yl)-2-(4-chloro-phenyl)acetamide (25).** mp 158−159 °C. ^{1}H NMR (400 MHz, CDCl$_3$): δ 1.34 (s, 9H, *tert*-butyl), 3.69 (s, 2H, CH$_2$), 6.56 (s, 1H, pyrazole), 7.09 (m, 3H, aromatic), 7.18 (s, 1H, NH), 7.25 (m, 4H, aromatic), 7.33 (m, 2H, aromatic). MS (CI): *m/e* 368 (MH$^+$). Anal. (C$_{21}$H$_{22}$ClN$_3$O) C, H, N.

Trifluoromethanesulfonic Acid 5-*tert*-Butyl-2-phenyl-*2H*-pyrazol-3-yl Ester (27). To a solution of 5-*tert*-butyl-2-phenyl-2,4-dihydro-pyrazol-3-one (**26**, 5.12 g, 23.7 mmol) and 2,6-di-*tert*-butyl-4-methyl pyridine (6.12 g, 29.8 mmol) in CH$_2$Cl$_2$ (50 mL) was added dropwise trifluoromethanesulfonic anhydride (4.4 mL, 7.4 g, 26 mmol) at −78 °C. The resulting solution was warmed to 0 °C, saturated NaHCO$_3$ solution (100 mL) was added, and the mixture was stirred vigorously for 10 min. The layers were separated, and the aqueous layer was extracted with CH$_2$Cl$_2$ (3×). The combined organic layers were washed with brine and dried (Na$_2$SO$_4$). Removal of the volatiles in vacuo provided a residue, which was purified by flash chromatography eluting unpolar impurities with hexanes and subsequently eluting the product with hexanes:ethyl acetate (20:1). Concentration in vacuo of the product-rich fractions gave 8.19 g (99%) of yellow oil **27**. ^{1}H NMR (400 MHz, CDCl$_3$): δ 1.34 (s, 9H, *tert*-butyl), 6.19 (s, 1H, pyrazole), 7.35 (dd, $^3J_1 = {}^3J_2 = 7.4$ Hz, 1H, phenyl), 7.4 (dd, $^3J_1 = {}^3J_2 = 7.8$ Hz, 2H, phenyl), 7.54 (d, 7.96 Hz, 2H, phenyl).

3-*tert*-Butyl-1-phenyl-5-vinyl-1*H*-pyrazole (28). A solution of **27** (3.74 g, 10.7 mmol) in dioxane (90 mL) in a sealable tube was degassed under vacuum and charged with nitrogen. LiCl (2.91 g, 68.8 mmol) was added, and the mixture was degassed and charged with nitrogen again. Pd(PPh$_3$)$_4$ (0.491 g, 0.425 mmol) was added, and the mixture was degassed and charged with nitrogen again. Tributyl(vinyl) tin (4.0 mL, 4.3 g, 14 mmol) was added, and the mixture was degassed and charged with nitrogen again. The tube was sealed, and the mixture was heated to 100 °C overnight. After it was cooled to room temperature, the volatiles were removed in vacuo and the residue was purified by flash chromatography eluting unpolar impurities with hexanes and subsequently eluting the product with hexanes in ethyl acetate (20:1). Concentration in vacuo of the product-rich fractions gave a residue, which was dissolved in ethyl acetate (100 mL) and stirred vigorously with saturated KF solution (30 mL). The organic layer was dried (Na$_2$SO$_4$). Removal of the volatiles in vacuo provided a residue, which was purified by flash chromatography using hexanes in ethyl acetate (20:1) as the eluent. Concentration in vacuo of the product-rich fractions gave 1.81 g (74%) of **28** as a yellow oil. ^{1}H NMR (400 MHz, CDCl$_3$): δ 1.37 (s, 9H, *tert*-butyl), 5.24 (dd, ^3J (Z) = 11.1, ^2J = 1.1 Hz, 1H, vinyl), 5.6 (dd, ^3J (E) = 17.5 Hz, ^2J = 1.1 Hz, 1H, vinyl), 6.4 (s, 1H, pyrazole), 6.51 (dd, ^3J (E) = 17.5, ^3J (Z) = 11.1 Hz, 1H, vinyl), 7.28−7.35 (m, 2H, phenyl), 7.39−7.45 (m, 3H, phenyl).

2-(5-*tert*-Butyl-2-phenyl-*2H*-pyrazol-3-yl)ethanol (29). To a solution of **28** (0.171 g, 0.756 mmol) in THF (20 mL) was added 9-BBN (1.9 mL of a 0.5 M solution in THF, 0.90 mmol) at 0 °C. After it was warmed to room temperature, the mixture was stirred overnight and heated to reflux for 4 h. Additional 9-BBN (0.8 mL of a 0.5 M solution in THF, 0.4 mmol) was added, and the mixture was heated to reflux for another 30 min. After it was cooled to room temperature, NaOH 10% (2.0 mL) and H$_2$O$_2$ (1.5 mL) were added and the mixture was stirred vigorously overnight. The reaction was diluted with water and Et$_2$O. The aqueous layer was extracted with ethyl ether (4×). The combined organic layers were washed with brine and dried (Na$_2$SO$_4$). Removal of the volatiles in vacuo provided a residue, which was purified by flash chromatography using 33% ethyl acetate in hexanes as the eluent. Concentration in vacuo of the product-rich fractions gave 0.133 g (72%) of **29** as a colorless oil. ^{1}H NMR (400 MHz, CDCl$_3$): δ 1.32 (s, 9H, *tert*-butyl), 2.72 (t, ^3J = 6.8 Hz, 2H, Ar−C*H$_2$*−CH$_2$−OH), 3.23 (s, broad, 1H, OH), 3.59 (t, ^3J = 6.8 Hz, 2H, Ar−CH$_2$−C*H$_2$*−OH), 6.07 (s, 1H, pyrazole), 7.26−7.39 (m, 5H, phenyl).

(5-*tert*-Butyl-2-phenyl-*2H*-pyrazol-3-yl)acetic Acid (30). To a solution of **29** (0.211 g, 0.865 mmol) in acetone (10 mL) was added dropwise Jones reagent at 0 °C until the orange color of the reagent persisted (approximately 0.5 mL). The mixture was stirred for 90 min at 0 °C and quenched with 2-propanol (1 mL). Water and ethyl ether were added, and the aqueous layer was extracted with ethyl ether (4×). The combined organic layers were dried (MgSO$_4$). Removal of the

volatiles in vacuo provided 0.220 g (98%) of white solid **30**. ^{1}H NMR (400 MHz, CDCl$_3$): δ 1.40 (s, 9H, *tert*-butyl), 3.58 (s, 2H, Ar−C**H**$_2$−COOH), 6.27 (s, 1H, pyrazole), 7.30−7.41 (m, 5H, phenyl), 9.51 (s (broad), 1H, COOH).

2-(5-*tert*-Butyl-2-phenyl-*2H*-pyrazol-3-yl)-*N*-(4-chloro-phenyl)acetamide (31). To a solution of **30** (0.220 g, 0.851 mmol) in CH$_2$Cl$_2$ (10 mL) at 0 °C was added DCC (0.315 g, 1.53 mmol), followed by DMAP (0.041 g (0.34 mmol) and 4-chloroaniline (0.212 g, 1.66 mmol). The mixture was stirred overnight, while it was warmed to room temperature, and quenched with the addition of NaHCO$_3$ solution (5 mL). The mixture was stirred vigorously for 1 h, and water was added. The organic layer was washed with 10% HCl (10 mL) and dried (Na$_2$SO$_4$). Removal of the volatiles in vacuo provided a residue, which was purified by flash chromatography using 25% ethyl acetate in hexanes as the eluent. Concentration in vacuo of the product-rich fractions gave 0.133 g (43%) of a white solid. The material was recrystallized from hexanes/ethyl acetate to give 0.093 g (30%) of **31** as a white solid; mp 186 °C. ^{1}H NMR (400 MHz, DMSO-d_6): δ 1.29 (s, 3H, *tert*-butyl), 3.81 (s, 2H, Ar−C**H**$_2$−C(O)NHAr), 6.33 (s, 1H, pyrazole), 7.35 (d, ^3J = 8.7 Hz, 2H, 4-chloro-phenyl) overlapping with 7.38 (dd, $^3J_1$ = $^3J_2$ = 7.0 Hz, 1H, phenyl), 7.49 (dd, $^3J_1$ = $^3J_2$ = 7.6 Hz, 2H, phenyl), 7.54 (d, ^3J = 7.6 Hz, 2H, phenyl), 7.59 (d, ^3J = 8.7 Hz, 2H, 4-chloro-phenyl), 10.29 (s, 1H, Ar−CH$_2$−C(O)N**H**Ar). MS (CI): *m/z* 368 (M + H)$^+$. Anal. (C$_{21}$H$_{22}$ClN$_3$O) C, H, N.

3-(5-*tert*-Butyl-2-phenyl-*2H*-pyrazol-3-yl)-1-(4-chlorophen-yl)-1-methyl-urea (34). To a solution of **15** (0.52 g, 2.4 mmol) in CH$_2$Cl$_2$ (25 mL) and aqueous saturated NaHCO$_3$ at 0 °C was added phosgene (2.5 mL of a 1.9 M solution in toluene, 4.8 mmol). The mixture was rapidly stirred for 10 min and extracted with CH$_2$Cl$_2$. The combined organic layers were dried (Na$_2$SO$_4$), and the volatiles were removed in vacuo to provide pyrazole isocyanate **32**, which was used without further purification. A solution of **32** (0.19 g, 0.80 mmol) and *N*-methyl-4-chloroaniline (**33**, 0.228 g, 1.61 mmol) in CH$_2$Cl$_2$ (3 mL) was stirred at room temperature overnight. Removal of the volatiles in vacuo provided a residue, which was purified by flash chromatography using 25% ethyl acetate in hexanes as the eluent. Concentration in vacuo of the product-rich fractions gave an oil, which was triturated with petroleum ether to give 0.075 g (24%) of **34**; mp 130−131 °C. ^{1}H NMR (400 MHz, CDCl$_3$): δ 1.32 (s, 9H, *tert*-butyl), 3.27 (s, 3H, N-Me), 6.41 (s, 1H, urea), 6.49 (s, 1H, pyrazole), 7.08−7.14 (m, 4H, aromatic), 7.27−7.32 (m, 5H, aromatic). Anal. (C$_{21}$H$_{23}$ClN$_4$O) C, H, N.

1-(5-*tert*-Butyl-2-phenyl-*2H*-pyrazol-3-yl)-3-(4-chlorophen-yl)-1-methyl-urea (37). A solution of **15** (2.13 g) in formic acid (7 mL) was heated to reflux for 4 h, cooled to room temperature, diluted with ethyl acetate, washed with aqueous NaHCO$_3$ and brine, and dried (Na$_2$SO$_4$). Removal of the volatiles in vacuo provided a residue, which was purified by flash chromatography using 20% ethyl acetate in hexanes as the eluent. Concentration in vacuo of the product-rich fractions gave 1.0 g (39%) of **35**. To a solution of **35** (0.398 g, 1.64 mmol) in THF (3 mL) at 0 °C was added BH$_3$-DMS (2.0 mL, 4.0 mmol) dropwise. After the addition was complete, the mixture was heated to reflux for 1.5 h, cooled to 0 °C, and quenched with methanol (1 mL). The mixture was stirred for 2.5 h, HCl (0.5 mL of a 4M solution in dioaxane) was added, and the mixture was heated to reflux for 1 h. After it was cooled to room temperature, methanol (5 mL) was added and the volatiles were removed in vacuo. The residue was basified (pH > 12) with 10% aqueous NaOH and extracted with ether. The combined extracts were dried (MgSO$_4$). Removal of the volatiles in vacuo provided 0.30 g (80%) of **36**. A mixture of **36** (0.15 g, 0.66 mmol) and 4-chlorophenyl isocyanate (0.10 g, 0.68 mmol) in CH$_2$Cl$_2$ (5 mL) was stirred at room temperature for 2 days. Removal of the volatiles in vacuo provided a solid, which was recrystallized from hexanes and ethyl acetate to give **37**; wt 0.16 g (63%); mp 153−154 °C. ^{1}H NMR (400 MHz, CDCl$_3$): δ 1.41 (s, 9H, *tert*-butyl), 3.06 (s, 3H, N-Me), 6.30 (s, 1H, pyrazole), 6.64 (s, 1H, urea), 7.20−7.25 (m, 4H, aromatic), 7.32−7.36 (m, 1H, aromatic), 7.43−7.50 (m, 4H, aromatic). Anal. (C$_{21}$H$_{23}$ClN$_4$O·0.25H$_2$O) C, H, N.

1-(5-*tert*-Butyl-2-phenyl-*2H*-pyrazol-3-yl)-3-indan-2-yl-urea (40). A solution of **32** (0.19 g, 0.81 mmol) and 2-amino-indan (**39**, 0.14 g, 1.1 mmol) in CH$_2$Cl$_2$ (5 mL) was stirred at room temperature overnight. Removal of the volatiles in vacuo provided a solid, which was recrystallized from hexanes and ethyl acetate to give **40**; wt 0.17 g (56%); mp 222−223 °C. ^{1}H NMR (400 MHz, CDCl$_3$): δ 1.32 (s, 9H, *tert*-butyl), 2.72 (dd, 2H, J = 4.6, 16.0 Hz, cyclopentyl), 3.26 (dd, 2H, J = 7.0, 16.0 Hz, cyclopentyl), 4.43−4.60 (m, 1H, cyclopentyl-CH−N), 5.11 (d, 1H, J = 7.4 Hz, urea), 6.12 (s, 1H, urea), 6.18 (s, 1H, pyrazole), 7.16−7.22 (m, 4H, aromatic), 7.31−7.38 (m, 1H, aromatic), 7.41−7.45 (m, 4H, aromatic). MS (NH$_3$-CI): *m/e* 375 (MH$^+$). Anal. (C$_{23}$H$_{26}$N$_4$O·0.25H$_2$O) C, H, N.

(4-Hydroxynaphthalen-1-yl)carbamic Acid *tert*-Butyl Ester (41). A solution of 4-amino-1-naphthol (1.88 g, 11.8 mmol) and di-*tert*-butyl dicarbonate (2.58 g, 11.8 mmol) in anhydrous THF (25 mL) was stirred overnight at room temperature, and the volatiles were removed in vacuo. The residue was purified with flash silica gel chromatography using 33% ethyl acetate in hexanes as the eluent. Concentration in vacuo of the product-rich fractions provided the solid product **41**.

[4-(2-Morpholin-4-yl-ethoxy)naphthalen-1-yl]carbam-ic Acid *tert*-Butyl Ester (42). A mixture of **41** (0.464 g, 1.69 mmol), 4-(2-chloroethyl)morpholine hydrochloride (0.345 g, 1.86 mmol), and powdered potassium carbonate (0.93 g, 6.75 mmol) in acetonitrile (15 mL) was heated at 80 °C for 3 h, cooled to room temperature, and diluted with ethyl acetate and water. The organic layer was washed with water and brine and dried (MgSO$_4$). Removal of the volatiles in vacuo provided a residue, which was purified by flash silica gel chromatog-raphy using 12% hexanes in ethyl acetate as the eluent. Concentration in vacuo of the product-rich fractions provided 0.528 g (84%) of the solid product **42**. ^{1}H NMR (270 MHz, CDCl$_3$): δ 8.25 (dd, 1H), 7.83 (d, 1H), 7.7−7.5 (m, 3H), 6.80 (d, 1H), 6.6 (bs, 1H), 4.30 (t, 2H), 3.75 (m, 4H), 2.92 (t, 2H), 2.61 (m, 4H), 1.55 (s, 9H). MS (CI): *m/e* 373 (MH$^+$).

1-Amino-4-(2-morpholin-4-yl-ethoxy)naphthalene Di-hydrochloride (43). A solution of **42** (0.511 g) and HCl (1 mL of a 4M solution in dioxane) in dioxane (5 mL) was stirred at room temperature for 20 h, and the volatiles were removed in vacuo. The residue was used without further purification. ^{1}H NMR (270 MHz, DMSO-d_6): δ 8.40 (d, 1H), 8.05 (d, 1H), 7.7 (m, 3H), 7.08 (d, 1H), 4.65 (m, 2H), 4.0−3.3 (m, 10H).

1-(5-*tert*-Butyl-2-*p*-tolyl-*2H*-pyrazol-3-yl)-3-[4-(2-mor-pholin-4-yl-ethoxy)naphthalen-1-yl]urea (45). To a mix-ture of **44** (prepared as in **15** using 4-methylphenyl hydrazine; ^{1}H NMR (270 MHz, DMSO-d_6): δ 7.5−7.4 (m, 4H), 5.6 (s, 1H), 2.33 (s, 3H), 1.25 (s, 9H)) (0.15 g, 0.56 mmol) in CH$_2$Cl$_2$ (15 mL) and saturated aqueous NaHCO$_3$ (15 mL) at 0 °C was added phosgene (1.2 mL of a 1.9 M solution in toluene, 2.25 mmol). The mixture was stirred rapidly for 15 min, and the organic layer was dried (MgSO$_4$). Most of the volatiles were removed in vacuo, and the residue was added to a solution of aminonaphthalene **43** (0.213 g, 0.620 mmol) and di-*iso*-propylethylamine (0.32 mL, 1.86 mmol) in anhydrous THF (10 mL). The mixture was stirred overnight at room temperature and diluted with water and ethyl acetate. The organic layer was washed with water and brine and dried (MgSO$_4$). Removal of the volatiles in vacuo provided a residue, which was purified by flash silica gel chromatography using ethyl acetate as the eluent. Concentration in vacuo of the product-rich fractions provided a solid, which was recrystallized with hexanes and ethyl acetate and provided 0.065 g (22%) of **45**; mp 142−143 °C. ^{1}H NMR (270 MHz, CDCl$_3$): δ 8.3 (m, 1H), 7.81 (m, 1H), 7.55 (m, 2H), 7.3 (d, 1H), 6.95 (m, 3H), 6.68 (d, 1H), 6.6 (bs, 1H), 6.48 (bs, 1H), 6.41 (s, 1H), 4,28 (t, 2H), 3.75 (m, 4H), 2.95 (t, 2H), 2.66 (m, 4H), 2.28 (s, 3H), 1.33 (s, 9H). MS (EI): *m/e* 527 (M$^+$). Anal. (C$_{31}$H$_{37}$N$_5$O$_3$) C, H, N.

1-(5-*tert*-Butyl-2-phenyl-*2H*-pyrazol-3-yl)-3-phenyl-urea (46). This compound was prepared similarly to **16** using phenyl isocyanate; mp 211 °C. ^{1}H NMR (400 MHz, DMSO-d_6): δ 1.29 (s, 9H, *tert*-butyl), 6.37 (s, 1H, pyrazole), 6.96−7.00 (m, 1H, aromatic), 7.24−7.27 (m, 2H, aromatic), 7.38−

7.41 (m, 3H, aromatic), 7.50–7.52 (m, 4H, aromatic), 8.39 (s, 1H, urea), 9.00 (s, 1H, urea). MS (NH₃-CI): *m/e* 335 (MH⁺). Anal. (C₂₀H₂₂N₄O) C, H, N.

1-(5-*tert*-Butyl-2-cyclohexyl-*2H*-pyrazol-3-yl)-3-phenyl Urea (47). To a solution of anhydrous hydrazine (0.36 mL, 11.6 mmol) in toluene (5 mL) at room temperature was added cyclohexanone (1.0 mL, 9.6 mmol) dropwise via syringe. After the addition, the mixture was heated to reflux for 30 min and cooled to 0 °C and absolute ethanol (5 mL), glacial acetic acid (15 mL), and sodium cyanoborohydride (0.728 g, 11.6 mmol) were added. The mixture was warmed to room temperature and stirred for 3.5 h. The mixture was diluted with 10% aqueous NaOH solution until a pH of 9–10 was reached (litmus) and extracted with chloroform. The combined extracts were dried (MgSO₄). Removal of the volatiles in vacuo afforded an oil and waxy solid (0.94 g) of cyclohexylhydrazine, which was used without further purifcation. A solution of cyclohexyl-hydrazine (0.94 g) and 4,4-dimethyl-3-oxo-pentanenitrile (1.21 g, 9.65 mmol) in ethanol (30 mL) was heated at reflux overnight and cooled to room temperature. Removal of the volatiles in vacuo provided a residue, which was purified by silica gel chromatography using 10–20% ethyl acetate in hexanes as the eluent. Concentration in vacuo of the product-rich fractions afforded 0.55 g of a mixture containing 4,4-dimethyl-3-oxo-pentanenitrile and 3-amino-5-*tert*-butyl-2-cyclohexyl-*2H*-pyrazole. This mixture and phenyl isocyanate (0.17 mL) in 3 mL of anhydrous THF was stirred at room temperature overnight. The solid was filtered, washed with CH₂Cl₂, and dried in vacuo to afford 0.25 g of **47**, which was recrystallized from methanol; mp 236 °C. ¹H NMR (400 MHz, DMSO-*d₆*): δ 1.21 (s, 9H, *tert*-butyl), 1.20–1.44 (m, 3H, cyclohexyl), 1.63–1.84 (m, 7H, cyclohexyl), 3.91–3.96 (m, 1H, cyclohexyl CH–N), 6.03 (s, 1 H, pyrazole C4–H), 6.98 (t, 1H, *J* = 7.3 Hz, phenyl C4–H), 7.28 (dd, 2H, *J* = 7.3 Hz, *J* = 7.7 Hz, phenyl-C3-H), 7.45 (d, 2H, *J* = 7.7 Hz, phenyl C2–H), 8.33 (s, 1H, urea), 8.82 (s, 1H, urea). MS (CI): *m/e* 341 (MH⁺). Anal. (C₂₀H₂₈N₄O) C, H, N.

1-(5-*tert*-Butyl-2-pyridin-4-yl-*2H*-pyrazol-3-yl)-3-phenyl-urea (57). This compound was prepared similarly to **16** using 4-hydrazinopyridine (prepared from 4-bromopyridine as in **52**);[46] mp 178–180 °C. ¹H NMR (400 MHz, CDCl₃): δ 1.25 (s, 9H, *tert*-butyl), 6.45 (s, 1 H, pyrazole), 7.08 (m, 1H, aromatic), 7.23 (m, 2H, aromatic), 7.31 (m, 2H, aromatic), 7.46 (m, 2H, aromatic), 7.92 (s, 1H, urea), 8.39 (m, 2H, aromatic), 8.47 (s, 1H, urea). MS (CI): *m/e* 336 (MH⁺). Anal. (C₁₉H₂₁N₅O) C, H, N.

1-(5-*tert*-Butyl-2-*o*-tolyl-*2H*-pyrazol-3-yl)-3-phenyl-urea (48). This compound was prepared from the condensation of *o*-tolylhydrazine and 4,4-dimethyl-3-oxo-pentanenitrile; see **50**; mp 180–182 °C. ¹H NMR (400 MHz, DMSO-*d₆*): δ 1.29 (s, 9H, *tert*-butyl), 1.9 (s, 3H, Ar–CH₃), 6.35 (s, 1 H, pyrazole C4–H), 6.95 (t, 1H, ArH), 7.29 (t, 2H, ArH), 7.35–7.5 (m, 6H, ArH), 8.18 (s, 1H, urea), 8.93 (s, 1H, urea). MS (CI): *m/e* 349 (MH⁺). Anal. (C₂₁H₂₄N₄O) C, H; N: calcd, 15.50; found, 16.08.

1-(5-*tert*-Butyl-2-*m*-tolyl-*2H*-pyrazol-3-yl)-3-phenyl-urea (49). This compound was prepared from the condensation of *m*-tolylhydrazine and 4,4-dimethyl-3-oxo-pentanenitrile; see **50**; mp 120–122 °C. ¹H NMR (400 MHz, DMSO-*d₆*): δ 1.28 (s, 9H, *tert*-butyl), 2.38 (s, 3H, Ar-*CH₃*), 6.38 (s, 1 H, pyrazole C4–H), 6.95 (t, 1H, ArH), 7.2–7.54 (m, 8H, ArH), 8.38 (s, 1H, urea), 9.04 (s, 1H, urea). MS (CI): *m/e* 349 (MH⁺). Anal. (C₂₁H₂₄N₄O) H, N; C: calcd, 72.39; found, 71.93.

1-(5-*tert*-Butyl-2-*p*-tolyl-*2H*-pyrazol-3-yl)-3-phenyl-urea (50). A solution of *p*-tolylhydrazine hydrochloride (3 g, 18.9 mmol), 4,4-dimethyl-3-oxopentanenitrile (2.6 g, 20.8 mmol), and concentrated HCl (2 mL) in ethanol (100 mL) was heated to reflux for 12 h, cooled to room temperature, basified with 20% aqueous NaOH to pH 12 (litmus), and extracted with ethyl acetate (3 × 20 mL). The combined organic layers were dried (MgSO₄). Removal of the volatiles in vacuo afforded 5-*tert*-butyl-2-*p*-tolyl-2H-pyrazol-3-yl-amine (**44**) as a yellow solid (3.7 g, 85%). A mixture of the above amine (0.150 g, 0.7 mmol) and phenyl isocyanate (0.07 mL, 0.7 mmol) in CH₂Cl₂ (10 mL) was stirred for 12 h at room temperature. Removal of

the volatiles in vacuo provided a residue, which was crystallized with ethyl acetate and hexanes and furnished the urea as a white solid (0.096 g, 42%); mp 179–180 °C. ¹H NMR (400 MHz, DMSO-*d₆*): δ 1.28 (s, 9H, *tert*-butyl), 2.38 (s, 3H, Ar–CH₃), 6.39 (s, 1 H, pyrazole C4–H), 6.95 (t, 1H, ArH), 7.22–7.5 (m, 8H, ArH), 8.35 (s, 1H, urea), 9.07 (s, 1H, urea). MS (CI): *m/e* 349 (MH⁺). Anal. (C₂₁H₂₄N₄O) C, H, N.

1-[5-*tert*-Butyl-2-(3,4-dimethylphenyl)-*2H*-pyrazol-3-yl]-3-phenyl-urea (51). This compound was prepared from 3,4-dimethylphenylhydrazine and 4,4-dimethyl-3-oxo-pentanenitrile as in **16**; mp 235–237 °C. ¹H NMR (400 MHz, DMSO-*d₆*): δ 1.25 (s, 9H, *tert*-butyl), 2.27 (s, 6H, 2xCH₃), 6.33 (s, 1H), 6.94 (t, ³*J* = 7.3 Hz, 1H, aromatic), 7.17–7.30 (m, 5H, aromatic), 7.37 (d, ³*J* = 7.6 Hz, 2H, aromatic), 8.30 (s, 1H, urea N–H), 9.00 (s, 1H, urea N–H). MS (CI): *m/e* 363 (MH⁺). Analysis (C₂₂H₂₆N₄O) C, H, N.

1-(5-*tert*-Butyl-2-naphthalen-2-yl-*2H*-pyrazol-3-yl)-3-phenyl-urea (52). This compound was prepared from 4,4-dimethyl-3-oxo-pentanenitrile and 2-naphthylhydrazine (from 2-bromonaphthalene as follows: To a solution of 2-bromonaph-thalene (2.00 g, 9.66 mmol) in THF (10 mL) at −78 °C was added dropwise *s*-BuLi (8.17 mL of a 1.3 M solution in cyclohexane, 10.62 mmol). The green mixture was stirred for 30 min and di-*tert*-butyl diazodicarboxylate (3.34 g, 14.5 mmol) was added slowly over 2 min. The reaction was warmed to room temperature, stirred overnight, quenched with water (10 mL), and extracted with CH₂Cl₂ (3 × 75 mL). The combined organic extracts were washed with brine and dried (Na₂SO₄). Removal of the volatiles in vacuo provided a residue, which was triturated with petroleum ether and afforded 1,2-di-(1,1-dimethylethoxycarbonyl)-1-naphth-2-yl-hydrazine as a pale orange solid (1.14 g). A mixture of 1,2-di-(1,1-dimethylethoxy-carbonyl)-1-naphth-2-yl-hydrazine (1.00 g, 2.79 mmol) and HCl (7.0 mL of a 4 M solution in dioxane) in 2-propanol (15 mL) was heated at 60 °C for 30 min, cooled to room temperature, and diluted with ethyl ether. Filtration and drying the solid in vacuo provided 0.42 g of 2-naphthylhydrazine hydrochloride as a yellow solid;[46] mp 229–230 °C. ¹H NMR (400 MHz, DMSO-*d₆*): δ 1.29 (s, 9H, *tert*-butyl), 6.43 (s, 1H, pyrazole 4-H), 6.94 (t, ³*J* = 7.3 Hz, 1H, aromatic), 7.23 (dd, ³*J₁* = ³*J₂* = 8.0 Hz, 2H, aromatic), 7.37 (d, ³*J* = 7.6 Hz, 2H, aromatic), 7.58 (m, 2H, aromatic), 7.67 (dd, ³*J* = 8.7 Hz, ⁴*J* = 2.0 Hz, 1H, aromatic), 8.00 (m, 2H, aromatic), 8.06 (m, 2H, aromatic), 8.50 (s, 1H, urea N–H), 9.00 (s, 1H, urea N–H). MS (CI): *m/e* 385 (MH⁺). Anal. (C₂₄H₂₄N₄O) C, H, N.

1-[2-(3-Aminophenyl)-5-*tert*-butyl-*2H*-pyrazol-3-yl]-3-phenyl-urea (53). A solution of 3-nitro-phenylhydrazine hydrochloride (2.0 g, 10.5 mmol), 4,4-dimethyl-3-oxopentane-nitrile (1.45 g, 11.6 mmol), and concentrated HCl (2 mL) in ethanol (100 mL) was heated to reflux for 12 h, cooled to room temperature, basified with 20% aqueous NaOH to pH 12 (litmus), and extracted with ethyl acetate (3 × 20 mL). The combined extracts were dried (MgSO₄). Removal of the vola-tiles in vacuo afforded 2-(3-nitrophenyl)-5-*tert*-butyl-2H-pyr-azol-3-yl-amine as a yellow solid (1.9 g, 70%). A mixture of this amine (0.40 g, 1.5 mmol) and phenyl isocyanate (0.184 mL, 1.7 mmol) in CH₂Cl₂ (10 mL) was stirred for 12 h at room temperature. Removal of the volatiles in vacuo provided a residue, which was crystallized with ethyl acetate and hexanes and furnished 1-[5-*tert*-butyl-2-(3-nitro-phenyl)-2H-pyrazol-3-yl]-3-phenyl-urea as a white solid (0.54 g, 92%). A mixture of this urea (0.4 g, 1.0 mmol), 10% Pd/C (0.08 g), and ammonium formate (0.4 g, 6.0 mmol) in ethanol (20 mL) was heated at 100 °C for 1 h, cooled to room temperture, and filtered through a plug of Celite. Removal of the volatiles in vacuo provided **53** (0.34 g, 98%); mp 150–151 °C. ¹H NMR (400 MHz, DMSO-*d₆*): δ 1.29 (s, 9H, *tert*-butyl), 5.41 (s, 2H, Ar-*NH₂*), 6.36 (s, 1 H, pyrazole C4–H), 6.55–6.72 (m, 3H, ArH), 6.99 (t, 1H, ArH), 7.15 (t, 1H, ArH), 7.28 (t, 3H, ArH), 7.43 (d, 2H, ArH), 8.35 (s, 1H, urea), 9.11 (s, 1H, urea). MS (CI): *m/e* 350 (MH⁺). Anal. (C₂₀H₂₃N₅O) C, H, N.

1-[2-(4-Aminophenyl)-5-*tert*-butyl-*2H*-pyrazol-3-yl]-3-phenyl-urea (54). mp 199–201 °C. ¹H NMR (400 MHz, DMSO-*d₆*): δ 1.28 (s, 9H, *tert*-butyl), 5.41 (s, 2H, Ar-*NH₂*), 6.31

(s, 1 H, pyrazole C4–H), 6.7 (d, 2H, ArH), 6.98 (t, 1H, ArH), 7.11 (d, 2H, ArH), 7.27 (t, 2H, ArH), 7.42 (d, 2H, ArH) 8.28 (s, 1H, urea), 9.15 (s, 1H, urea). Anal. ($C_{20}H_{23}N_5O$) C, N; H: calcd, 7.12; found, 6.68.

1-(5-Methyl-2-phenyl-*2H*-pyrazol-3-yl)-3-phenyl-urea (58). mp 195 °C. ^{1}H NMR (400 MHz, DMSO-d_6): δ 2.20 (s, 3H, methyl), 6.29 (s, 1H, pyrazole), 6.95–6.99 (m, 1H, aromatic), 7.25–7.29 (m, 2H, aromatic), 7.39–7.44 (m, 3H, aromatic), 7.51–7.56 (m, 4H, aromatic), 8.42 (s, 1H, urea), 8.98 (s, 1H, urea). MS (PB–NH$_3$–CI): *m/e* 293 (MH$^+$). Anal. ($C_{17}H_{16}N_4O$) C, H, N.

1-(5-Isopropyl-2-phenyl-*2H*-pyrazol-3-yl)-3-phenyl-urea (59). This compound was prepared as in **23** using methyl isobutyrate; mp 161 °C. ^{1}H NMR (400 MHz, DMSO-d_6): δ 1.23 (d, 6H, $J = 6.9$ Hz, (CH$_3$)$_2$C-), 2.84–2.94 (m, 1H, Me$_2$CH), 6.34 (s, 1H, pyrazole), 6.95–6.99 (m, 1H, aromatic), 7.24–7.33 (m, 2H, aromatic), 7.39–7.45 (m, 3H, aromatic), 7.51–7.56 (m, 4H, aromatic), 8.42 (s, 1H, urea), 9.01 (s, 1H, urea). MS (EI): *m/e* 320 (M$^+$). Anal. ($C_{19}H_{20}N_4O$) C, H, N.

1-[5-(1,1-Dimethylpropyl)-2-phenyl-*2H*-pyrazol-3-yl]-3-phenyl-urea (60). This compound was prepared as in **20** using 2,2-dimethylbutyric acid; mp 175 °C. ^{1}H NMR (400 MHz, DMSO-d_6): δ 0.79 (t, 3H, propyl C3–H), 1.23 (s, 6H, dimethyl), 1.60 (q, 2H, propyl C2–H), 6.35 (s, 1H, pyrazole), 6.95–6.99 (m, 1H, aromatic), 7.24–7.28 (m, 2H, aromatic), 7.39–7.44 (m, 3H, aromatic), 7.51–7.57 (m, 4H, aromatic), 8.41 (s, 1H, urea), 9.02 (s, 1H, urea). MS (NH$_3$–CI): *m/e* 349 (MH$^+$). Anal. ($C_{21}H_{24}N_4O$) C, H, N.

1-[5-(2-Methoxy-1,1-dimethylethyl)-2-phenyl-*2H*-pyrazol-3-yl]-3-phenyl-urea (61). This compound was prepared as in **23** using methyl 2,2-dimethyl-3-methoxypropionate. Foam, softens 68–72 °C. ^{1}H NMR (400 MHz, DMSO-d_6): δ 1.26 (s, 6H, dimethyl), 3.27 (s, 3H, CH$_3$O-), 3.39 (s, 2H, CCH$_2$–O), 6.38 (s, 1H, pyrazole), 6.95–6.99 (m, 1H, aromatic), 7.25–7.28 (m, 2H, aromatic), 7.39–7.44 (m, 3H, aromatic), 7.52–7.57 (m, 4H, aromatic), 8.40 (s, 1H, urea), 9.01 (s, 1H, urea). MS (NH$_3$–CI): *m/e* 365 (MH$^+$). Anal. ($C_{21}H_{24}N_4O_2$) C, H, N.

1-(5-Cyclohexyl-2-phenyl-*2H*-pyrazol-3-yl)-3-phenyl-urea (62). mp 182 °C. ^{1}H NMR (400 MHz, DMSO-d_6): δ 1.16–1.20 (m, 1H, cyclohexyl), 1.22–1.47 (m, 4H, cyclohexyl), 1.67–1.70 (br d, 1H, $J = 12.2$ Hz, cyclohexyl), 1.76–1.79 (br d, 2H, $J = 12.1$ Hz, cyclohexyl), 1.92–1.95 (br d, 2H, $J = 10.7$ Hz, cyclohexyl), 2.54–2.60 (m, 1H, cyclohexyl), 6.31 (s, 1H, pyrazole), 6.95–6.99 (m, 1H, aromatic), 7.24–7.28 (m, 2H, aromatic), 7.39–7.43 (m, 3H, aromatic), 7.51–7.55 (m, 4H, aromatic), 8.40 (s, 1H, urea), 9.00 (s, 1H, urea). MS (PB-EI): *m/e* 360 (M·). Anal. ($C_{22}H_{24}N_4O$) C, H, N.

1-[5-(1-Methyl-1-phenylethyl)-2-phenyl-*2H*-pyrazol-3-yl]-3-phenyl-urea (64). Ethyl phenyl acetate (4.0 mL, 25.1 mmol) in 100 mL of anhydrous THF was added dropwise to a −78 °C solution of lithium hexamethyldisilyl amide (30.1 mL of a 1.0 M solution in THF). After 30 min, iodomethane (30.1 mmol, 1.9 mL) was added and the mixture was stirred for 30 min, warmed to room temperature, and stirred for 4 h. The mixture was quenched with a saturated aqueous solution of NH$_4$Cl and extracted with ethyl acetate. The combined organic extracts were washed with Na$_2$S$_2$O$_3$ solution and brine and dried (MgSO$_4$). Removal of the volatiles in vacuo provided a residue, which was subjected without purification to the same conditions described above to introduce the second methyl group. Purification by silica gel chromatography afforded 4.05 g (84%) of ethyl 2-methyl-2-phenylpropionate. A mixture of this ester (0.370 g, 1.93 mmol) and anhydrous acetonitrile (0.14 mL, 2.70 mmol) in anhydrous toluene (4.0 mL) was added dropwise to NaH (0.088 g of 60% dispersed in mineral oil, 2.20 mmol) in toluene (3 mL) at reflux. The mixture was heated for 2 h, cooled to room temperature, carefully quenched with 5 N aqueous HCl, and extracted with CH$_2$Cl$_2$ (3 × 5 mL). The combined organic extracts were dried (MgSO$_4$). Removal of the volatiles in vacuo provided a 1:1 mixture of starting ethyl propionate and desired β-keto-nitrile product. Without any purification, this material and phenyl hydrazine (0.2 mL, 1.9 mmol) in toluene (12 mL) were heated to reflux overnight and cooled to room temperature. Removal of the volatiles in vacuo

provided a residue, which was purified by silica gel chromatography using 30% ethyl acetate in hexanes as the eluent. Concentration in vacuo of the product-rich fractions provided (0.121 g, 23%) of 3-amino-5-(1-methyl-1-phenylethyl)-2-phenyl-*2H*-pyrazole as an orange solid. A mixture of this amino-pyrazole and phenyl isocyanate (50 uL, 0.436 mmol) in anhydrous THF (2 mL) was stirred at room temperature under inert atmosphere overnight. Removal of the volatiles in vacuo provided a residue, which was purified by silica gel chromatography using 1–5% methanol in CH$_2$Cl$_2$ as the eluent. Concentration in vacuo of the product-rich fractions provided **64** as a light tan foam, which softens at 81–83 °C. ^{1}H NMR (400 MHz, DMSO-d_6): δ 1.67 (s, 6H, dimethyl), 6.25 (s, 1H, pyrazole), 6.94–6.98 (m, 1H, aromatic), 7.12–7.20 (m, 1H, aromatic), 7.23–7.32 (m, 4H, aromatic), 7.36–7.39 (m, 4H, aromatic), 7.42–7.47 (m, 1H, aromatic), 7.55–7.59 (m, 4H, aromatic), 8.44 (s, 1H, urea), 9.02 (s, 1H, urea). MS (EI): *m/e* 397 (MH$^+$). Anal. ($C_{25}H_{24}N_4O$) C, H, N.

1-(5-*tert*-Butyl-2-phenyl-*2H*-pyrazol-3-yl)-3-cyclohexyl-urea (66). This compound was prepared as in **40** using cyclohexylamine; mp 206 °C. ^{1}H NMR (400 MHz, DMSO-d_6): δ 1.10–1.20 (m, 5H, cyclohexyl), 1.28 (s, 9H, *tert*-butyl), 1.48–1.51 (m, 1H, cyclohexyl), 1.61–1.64 (m, 2H, cyclohexyl), 1.75–1.79 (m, 2H, cyclohexyl), 3.36–3.41 (m, 1H, cyclohexyl-CH–N), 6.26 (s, 1H, pyrazole), 6.48 (d, 1H, urea), 7.35–7.40 (m, 1H, aromatic), 7.42–7.51 (m, 4H, aromatic), 8.00 (s, 1H, urea). MS (NH$_3$–CI): *m/e* 341 (MH$^+$). Anal. ($C_{20}H_{28}N_4O$) C, H, N.

1-(5-*tert*-Butyl-2-phenyl-2*H*-pyrazol-3-yl)-3-(2,3-dimethylphenyl)-urea (72). This compound was prepared as in **40** using 2,3-dimethylaniline; mp 210–213 °C. ^{1}H NMR (400 MHz, CDCl$_3$): δ 1.37 (s, 9H, *tert*-butyl), 2.06 (s, 3H, CH$_3$), 2.26 (s, 3H, CH$_3$), 6.40 (s, 1H, urea), 6.44 (s, 1H, pyrazole), 6.45 (s, 1H, urea), 7.06 (m, 2H, aromatic), 7.18 (m, 1H, aromatic), 7.36 (m, 5H, aromatic). MS (CI): *m/e* 363 (MH$^+$). Anal. ($C_{22}H_{26}N_4O$) C, H, N.

1-Benzyl-3-(5-*tert*-butyl-2-phenyl-*2H*-pyrazol-3-yl)-urea (73). This compound was prepared as in **40** using benzylamine; mp 190–192 °C. ^{1}H NMR (400 MHz, CDCl$_3$): δ 1.35 (s, 9H, *tert*-butyl), 4.40 (d, 2H, $J = 5.8$ Hz, benzyl-CH$_2$), 5.19–5.22 (m, 1H, urea), 6.14 (s, 1H, urea), 6.27 (s, 1H, pyrazole), 7.18–7.19 (m, 1H, aromatic), 7.26–7.37 (m, 4H, aromatic), 7.42–7.49 (m, 5H, aromatic). MS (NH$_3$–CI): *m/e* 349 (MH$^+$). Anal. ($C_{21}H_{24}N_4O$) C, H, N.

1-(5-*tert*-Butyl-2-phenyl-*2H*-pyrazol-3-yl)-3-phenethyl-urea (74). This compound was prepared as in **40** using phenethylamine; mp 144–146 °C. ^{1}H NMR (400 MHz, CDCl$_3$): δ 1.32 (s, 9H, *tert*-butyl), 2.81 (t, 2H, $J = 6.7$ Hz, benzylic-CH$_2$), 3.49–3.54 (m, 2H, N–CH$_2$-benzyl), 4.92–4.95 (m, 1H, urea), 6.03 (s, 1H, pyrazole), 7.17–7.18 (m, 2H, aromatic), 7.23–7.38 (m, 4H, aromatic), 7.44–7.47 (m, 4H, aromatic). MS (NH$_3$–CI): *m/e* 363 (MH$^+$). Anal. ($C_{22}H_{26}N_4O$) C, H, N.

1-(5-*tert*-Butyl-2-phenyl-*2H*-pyrazol-3-yl)-3-indan-1-yl-urea (77). This compound was prepared as in **40** using racemic 1-aminoindan; mp 171–173 °C. ^{1}H NMR (400 MHz, CDCl$_3$): δ 1.34 (s, 9H, *tert*-butyl), 1.63–1.73 (m, 1H, cyclopentyl), 2.53–2.60 (m, 1H, cyclopentyl), 2.79–2.96 (2 m, 2H, cyclopentyl), 5.03 (d, 1H, $J = 8.4$ Hz, urea), 5.33 (dd, 1H, $J = 15.8, 8.0$ Hz, cyclopentyl-CH–N), 6.13 (s, 1H, urea), 6.27 (s, 1H, pyrazole), 7.11–7.13 (m, 1H, aromatic), 7.17–7.21 (m, 1H, aromatic), 7.22–7.24 (m, 2H, aromatic), 7.35–7.38 (m, 1H, aromatic), 7.45–7.49 (m, 2H, aromatic), 7.51–7.54 (m, 2H, aromatic). MS (NH$_3$–CI): *m/e* 375 (MH$^+$). Anal. ($C_{23}H_{26}N_4O$) C, H, N.

1-(5-*tert*-Butyl-2-*p*-tolyl-2*H*-pyrazol-3-yl)-3-(2-fluorophenyl)-urea (78). A mixture of 5-*tert*-butyl-2-*p*-tolyl-2*H*-pyrazol-3-yl-amine (**44**, 0.10 g, 0.4 mmol) and 2-fluorophenyl isocyanate (0.053 mL, 0.5 mmol) in CH$_2$Cl$_2$ (10 mL) was stirred for 12 h at room temperature. Removal of the volatiles in vacuo provided a residue, which was crystallized with ethyl acetate and hexanes and furnished the urea as a white solid (0.093 g, 58%); mp 103–104 °C. ^{1}H NMR (400 MHz, DMSO-d_6): δ 1.29 (s, 9H, *tert*-butyl), 2.39 (s, 3H, Ar-*CH$_3$*), 6.41 (s, 1 H, pyrazole

C4−H), 6.95−7.55 (m, 7H, ArH), 8.84 (s, 1H, urea), 8.98 (s, 1H, urea). MS (CI): m/e 367 (MH$^+$). Anal. (C$_{21}$H$_{23}$FN$_4$O) C, H, N.

Biological Methods

Plate Assay for Estimating Binding Affinity (K_d) of Compounds for p38 MAP Kinase. Fluorescence Binding Assay. The binding affinities for inhibitors of human recombinant p38 MAP kinase[59] were determined using a simple fluorescent binding assay. The assay is based upon competition between a fluorescent probe SK&F 86002 and any inhibitor of choice. Inhibitors were assayed at two concentrations, typically 1 and 0.1 μM. The actual concentrations of compounds were verified by an analytical high-performance liquid chromatography (HPLC). Compounds were diluted into binding buffer (20 mM Bis-TRIS Propane, pH 7.0, 2 mM EDTA, 0.01% sodium azide, and 0.15% octylglucoside) and placed in a 96 well fluorescent microtiter plate. Fluoroprobe was added followed by the addition of p38 MAP kinase. The plate was incubated at room temperature for 60 min. Plates are read in a fluorescent microtiter plate reader using an excitation wavelength of 332 nm and an emission wavelength of 420 nm. The assay was run in duplicate; all 48 data points (3 × 8 data points in duplicate) were fit simultaneously to a simple equilibrium binding equation, which results in an estimation of binding affinity or K_d. In all cases, standard errors and P values were within statistically acceptable limits. A standard compound was included with each set of experiments and its K_d varied by ±25%.

THP-1 Cell Assay for Inhibition of LPS-Induced TNF-α Production. Cell Culture and Compound Preparation. THP-1 cells (ATCC TIB 202, American Type Culture Collection, Rockville, MD) were maintained at 37 °C, 5% CO$_2$ in 10% fetal bovine serum (FBS)/RPMI 1640 media as previously described.[45] The day of the assay, cells and reagents were diluted in 3% FBS/RPMI 1640 media. Test compounds in DMSO were diluted into 3% FBS/RPMI 1640 media and centrifuged at room temperature for 10 min at 12 000g to precipitate any undissolved compound. The actual concentration of dissolved compound was determined by an HPLC method. Supernatant was diluted serially in 3% FBS/ RPMI 1640 media containing 0.4% DMSO for all subsequent dilutions (0.2% DMSO final).

THP-1 Cell Assay. Confluent THP-1 cells (2 × 10^6 cells/mL, final concentration) were added to culture plates containing test compound or DMSO vehicle. The cell mixture was allowed to preincubate for 30 min at 37 °C, 5% CO$_2$, prior to stimulation with LPS (Sigma L-2630, from *Escherichia coli* serotype 0111.B4; 1 ug/ mL final). Blanks (unstimulated) received H$_2$O vehicle. Overnight incubation (18−24 h) proceeded as described above. The assay was terminated by centrifuging the plates for 5 min at room temperature at 400g; supernatants were transferred to clean culture plates and stored at −80 °C until analyzed for human TNF-α by a commercially available enzyme-linked immunosorbent assay (ELISA) kit (Biosource #KHC3012, Camarillo, CA).

Data Analysis. The data from two or greater individual assays were combined and analyzed by nonlinear regression (SAS Software System, SAS institute, Inc., Cary, NC) to generate a dose response curve. A three

parameter logistic model was used of the form: percent inhibition = $I_{max} \times conc^N/conc^N + IC_{50}N$. The calculated IC$_{50}$ value is the concentration of the test compound that caused a 50% decrease in the maximal inhibition of p38 activity as measured by TNF-α production.

In Vivo LPS Challenge Assay. Female Balb/c mice, weighing approximately 20 gm, were used. Mice were administered **1**, test compound, and vehicle in cremophor (po) approximately 30 min prior to LPS/D-gal administration. The volume of oral gavage was 0.15 mL. Then, mice were administered LPS (*E. coli* LPS 0111: B4, 1.0 μg/mouse) plus D-gal (50 mg/kg) intravenously in 0.2 mL of pyrogen-free saline. One hour after LPS/ D-gal, each mouse was anesthetized, bled by cardiac puncture, and collected for serum TNF-α and compound levels. Blood samples were centrifuged at 2500 rpm for 10−15 min, the serum was decanted, and samples were stored frozen at −70 °C until transfer either for TNF-α determination or to Drug Metabolism and Pharmacokinetics for plasma concentration analysis by HPLC. The concentration of TNF-α in the serum was measured by a commercially available ELISA kit (R&D Systems, Minneapolis, MN). ELISA was performed according to the manufacturers assay procedure. All samples were assayed in duplicate.

X-ray Crystallography. Crystals of human p38MAP kinase in complex with inhibitors were prepared by the hanging drop vapor diffusion method.[59] The crystals belonged to the space group $P2(1)2(1)2(1)$ and are isomorphous to those reported for **45**.[45] X-ray diffraction data were collected at 100 K, and the structure refinement was carried out with the X-Plor program. An example is shown below for compound **75**. Space group, $P2(1)2(1)2(1)$; cell parameters (a,b,c), 65.4, 75.0, 78.7; maximum resolution, 2A; number of observations, 277 841; number of reflections, 26 717; completeness, 97; R_{merge}, 5.0%; R/free R factor, 21.4/29.1; rms deviation in bond lengths, 0.010; rms deviation in bond angles, 1.4.

References

(1) Dinarello, C. A. Inflammatory cytokines: interleukin-1 and tumor necrosis factor as effector molecules in autoimmune diseases. *Curr. Opin. Immunol.* **1991**, *3*, 941−948.
(2) Foster, M. L.; Halley, F.; Souness, J. E. Potential of p38 inhibitors in the treatment of rheumatoid arthritis. *Drug News Perspect.* **2000**, *13*, 488−497.
(3) Feldmann, M.; Brennan, F. M.; Maini, R. N. Role of cytokines in rheumatoid arthritis. *Annu. Rev. Immunol.* **1996**, *14*, 397−440.
(4) Jarvis, B.; Faulds, D. Etanercept: a review of its use in rheumatoid arthritis. *Drugs* **1999**, *57*, 945−966.
(5) Garrison, L.; McDonnell, N. D. Etanercept: therapeutic use in patients with rheumatoid arthritis. *Ann. Rheum. Dis.* **1999**, *58 (Suppl. 1)*, 65−169.
(6) Maini, R.; St. Clair, E. W.; Breedveld, F.; Furst, D.; Kalden, J.; Weisman, M.; Smolen, J.; Emery, P.; Harriman, G.; Feldmann, M.; Lipsky, P. Infliximab (chimeric anti-tumour necrosis factor alpha monoclonal antibody) versus placebo in rheumatoid arthritis patients receiving concomitant methotrexate: a randomised phase III trial. *Lancet* **1999**, *354*, 1932−1939.
(7) Carteron, N. L. Cytokines in rheumatoid arthritis: trials and tribulations. *Mol. Med. Today* **2000**, *6*, 315−323.

(8) Hamilton, K.; St. Clair, E. W. Tumour necrosis factor—alpha blockade: a new era for effective management of rheumatoid arthritis. *Exp. Opin. Ther. Pat.* **2000**, *1*, 1041–1052.

(9) Present, D. H.; Rutgeerts, P.; Targan, S.; Hanauer, S. B.; Mayer, L.; van Hogezand, R. A.; Podolsky, D. K.; Sands, B. E.; Braakman, T.; DeWoody, K. L.; Schaible, T. F.; van Deventer, S. J. Infliximab for the treatment of fistulas in patients with Crohn's disease. *N. Engl. J. Med.* **1999**, *340*, 1398–1405.

(10) Rutgeerts, P. J. Review article: efficacy of infliximab in Crohn's disease—induction and maintenance of remission. *Aliment. Pharmacol. Ther.* **1999**, *13 (Suppl 4)*, 9–15.

(11) Lee, J. C.; Laydon, J. T.; McDonnell, P. C.; Gallagher, T. F.; Kumar, S.; Green, D.; McNulty, D.; Blumenthal, M. J.; Heys, J. R.; Landvatter, S. W.; Strickler, J. E.; McLaughlin, M. M.; Siemens, I. R.; Fisher, S. M.; Livi, G. P.; White, J. R.; Adams, J. L.; Young, P. R. A protein kinase involved in the regulation of inflammatory cytokine biosynthesis. *Nature* **1994**, *372*, 739–746.

(12) Herlaar, E.; Brown, Z. p38 MAPK signalling cascades in inflammatory disease. *Mol. Med. Today* **1999**, *5*, 439–447.

(13) Ono, K.; Han, J. The p38 signal transduction pathway. Activation and function. *Cell. Signalling* **2000**, *12*, 1–13.

(14) Lee, J. C.; Kassis, S.; Kumar, S.; Badger, A.; Adams, J. L. p38 mitogen-activated protein kinase inhibitors-mechanisms and therapeutic potentials. *Pharmacol. Ther.* **1999**, *82*, 389–397.

(15) Lee, J. C.; Kumar, S.; Griswold, D. E.; Underwood, D. C.; Votta, B. J.; Adams, J. L. Inhibition of p38 MAP kinase as a therapeutic strategy. *Immunopharmacology* **2000**, *47*, 185–201.

(16) Henry, J. R.; Cavender, D. E.; Wadsworth, S. A. p38 Mitogen-Activated Protein Kinase as a Target for Drug Discovery. *Drugs Future* **1999**, *24*, 1345–1354.

(17) Salituro, F. G.; Germann, U. A.; Wilson, K. P.; Bemis, G. W.; Fox, T.; Su, M. S. Inhibitors of p38 MAP kinase: therapeutic intervention in cytokine-mediated diseases. *Curr. Med. Chem.* **1999**, *6*, 807–823.

(18) Boehm, J. C.; Smietana, J. M.; Sorenson, M. E.; Garigipati, R. S.; Gallagher, T. F.; Sheldrake, P. L.; Bradbeer, J.; Badger, A. M.; Laydon, J. T.; Lee, J. C.; Hillegass, L. M.; Griswold, D. E.; Breton, J. J.; Chabot-Fletcher, M. C.; Adams, J. L. 1-Substituted 4-aryl-5-pyridinylimidazoles: a new class of cytokine suppressive drugs with low 5-lipoxygenase and cyclooxygenase inhibitory potency. *J. Med. Chem.* **1996**, *39*, 3929–3937.

(19) Adams, J. L.; Boehm, J. C.; Gallagher, T. F.; Kassis, S.; Webb, E.; Hall, R.; Sorenson, M.; Garigipati, R. S.; Griswold, D. E.; Lee, J. C. Pyrimidinylimidazole inhibitors of p38: Cyclic N-1 imidazole substituents enhance p38 kinase inhibition and oral activity. *Bioorg. Med. Chem. Lett.* **2001**, *11*, 2867–2870.

(20) Boehm, J. C.; Bower, M. J.; Gallagher, T. F.; Kassis, S.; Johnson, S. R.; Adams, J. L. Phenoxypyrimidine inhibitors of p38 kinase: Synthesis and statistical evaluation of the p38 inhibitory potencies of a series of 1-(piperdin-4-yl)-4-(4-fluorophenyl)-5-(2-phenoxypyrimidin-4-yl) imidazoles. *Bioorg. Med. Chem. Lett.* **2001**, *11*, 1123–1126.

(21) Adams, J. L.; Boehm, J. C.; Kassis, S.; Gorycki, P. D.; Webb, E. F.; Hall, R.; Sorenson, M.; Lee, J. C.; Ayrton, A.; Griswold, D. E.; Gallagher, T. F. Pyrimidinylimidazole inhibitors of CSBP/p38 kinase demonstrating decreased inhibition of hepatic cytochrome P450 enzymes. *Bioorg. Med. Chem. Lett.* **1998**, *8*, 3111–3116.

(22) Adams, J. L.; Boehm, J. C.; Gallagher, T. F.; Kassis, S.; Webb, E. F.; Hall, R.; Sorenson, M.; Garigipati, R.; Griswold, D. E.; Lee, J. C. Pyrimidinylimidazole inhibitors of p38: cyclic N-1 imidazole substituents enhance p38 kinase inhibition and oral activity. *Bioorg. Med Chem. Lett.* **2001**, *11*, 2867–2870.

(23) Badger, A. M.; Bradbeer, J. N.; Votta, B.; Lee, J. C.; Adams, J. L.; Griswold, D. E. Pharmacological profile of SB 203580, a selective inhibitor of cytokine suppressive binding protein/p38 kinase, in animal models of arthritis, bone resorption, endotoxin shock and immune function. *J. Pharmacol. Exp. Ther.* **1996**, *279*, 1453–1461.

(24) Fullerton, T.; Sharma, A.; Prabhakar, U.; Tucci, M.; Boike, S.; Davis, H.; Jorkasky, D.; Williams, W. Suppression of ex-vivo cytokine production by SB-242235, a selective inhibitor of p38 MAP kinase. *Clin. Pharmacol. Ther.* **2000**, *67*, 114; Abstract OI-B-4.

(25) Hanson, G. J. Inhibitors of p38 Kinase. *Exp. Opin. Ther. Pat.* **1997**, *7*, 729–733.

(26) Boehm, J. C.; Adams, J. L. New inhibitors of p38 kinase. *Exp. Opin. Ther. Pat.* **2000**, *10*, 25–37.

(27) Dumas, J. Protein kinase inhibitors: emerging pharmacophores 1997–2000. *Exp. Opin. Ther. Pat.* **2001**, *11*, 405–429.

(28) Liverton, N. J.; Butcher, J. W.; Claiborne, C. F.; Claremon, D. A.; Libby, B. E.; Nguyen, K. T.; Pitzenberger, S. M.; Selnick, H. G.; Smith, G. R.; Tebben, A.; Vacca, J. P.; Varga, S. L.; Agarwal, L.; Dancheck, K.; Forsyth, A. J.; Fletcher, D. S.; Frantz, B.; Hanlon, W. A.; Harper, C. F.; Hofsess, S. J.; Kostura, M.; Lin, J.; Luell, S.; O'Neill, E. A.; Orvello, C. J.; Pang, M.; Parsons, J.;

(29) McLay, I. M.; Halley, F.; Souness, J. E.; McKenna, J.; Benning, V.; Birrell, M.; Burton, B.; Belvisi, M.; Collis, A.; Constan, A.; Foster, M.; hele, D.; Jayyosi, Z.; Kelley, M.; Maslen, C.; Miller, G.; Ouldelhkim, M.-C.; Page, K.; Phipps, S.; Pollock, K.; Porter, B.; Ratcliffe, A. J.; Redford, E. J.; Webber, S.; Slater, B.; Thybaud, V.; Wilsher, N. The discovery of RPR 200765A, a p38 MAP kinase inhibitor displaying a good oral antiarthritic efficacy. *Bioorg. Med. Chem.* **2001**, *9*, 537–554.

(30) de Laszlo, S. E.; Visco, D.; Agarwal, L.; Chang, L.; Chin, J.; Croft, G.; Forsyth, A.; Fletcher, D.; Frantz, B.; Hacker, C.; Hanlon, W.; Harper, C.; Kostura, M.; Li, B.; Luell, S.; MacCoss, M.; Mantlo, N.; O'Neill, E. A.; Orevillo, C.; Pang, M.; Parsons, J.; Rolando, A.; Sahly, Y.; Sidler, K.; Widmer, W. R.; O'Keefe, S. J. Pyrroles and other heterocycles as inhibitors of p38 kinase. *Bioorg. Med. Chem. Lett.* **1998**, *8*, 2689–2694.

(31) Revesz, L.; Di Padova, F. E.; Buhl, T.; Feifel, R.; Gram, H.; Hiestand, P.; Manning, U.; Zimmerlin, A. G. SAR of 4-hydroxy-piperidine and hydroxyalkyl substituted heterocycles as novel p38 map kinase inhibitors. *Bioorg. Med. Chem. Lett.* **2000**, *10*, 1261–1264.

(32) Henry, J. R.; Rupert, K. C.; Dodd, J. H.; Turchi, I. J.; Wadsworth, S. A.; Cavender, D. E.; Fahmy, B.; Olini, G. C.; Davis, J. E.; Pellegrino-Gensey, J. L.; Schafer, P. H.; Siekierka, J. J. 6-Amino-2-(4-fluorophenyl)-4-methoxy-3-(4-pyridyl)-1H-pyrrolo-[2,3-b]pyridine (RWJ 68354): a potent and selective p38 kinase inhibitor. *J. Med. Chem.* **1998**, *41*, 4196–4198.

(33) Wadsworth, S. A.; Cavender, D. E.; Beers, S. A.; Lalan, P.; Schafer, P. H.; Malloy, E. A.; Wu, W.; Fahmy, B.; Olini, G. C.; Davis, J. E.; Pellegrino-Gensey, J. L.; Wachter, M. P.; Siekierka, J. J. RWJ 67657, a potent, orally active inhibitor of p38 mitogen-activated protein kinase. *J. Pharmacol. Exp. Ther.* **1999**, *291*, 680–687.

(34) Fijen, J. W.; Zijlstra, J. G.; De Boer, P.; Spanjersberg, R.; Cohen Tervaert, J. W.; Van Der Werf, T. S.; Ligtenberg, J. J.; Tulleken, J. E. Suppression of the clinical and cytokine response to endotoxin by RWJ-67657, a p38 mitogen-activated protein-kinase inhibitor, in healthy human volunteers. *Clin. Exp. Immunol.* **2001**, *124*, 16–20.

(35) Salituro, F. G.; Bemis, G. W.; Germann, U. A.; Duffy, J. P.; Galullo, V. P.; Gao, H.; Harrington, E. M.; Wilson, K. P.; Su, M. S.-S. Discovery of VX-745: A novel orally bioavailable and selective p38 MAP kinase inhibitor. Proceedings of the 27th National Medicinal Chemistry Symposium, Kansas City, MO, June 13, 2000; S-03.

(36) Vertex patent application WO 9958502 (Nov 18, 1999).

(37) Goldstein, D. The discovery of RO3201195, a novel and selective inhibitor of p38 kinase. Fifth World Conference on Inflammation, Edinburgh, Scotland, September 22–26, 2001; Abstract 12/02.

(38) Hoffmann-LaRoche patent application WO 0129042 (April 26, 2001).

(39) Scios, Inc. patent application WO 0012074 (March 9, 2000).

(40) Aaes, H.; Skak-Nielsen, T.; Hansen, J. R.; Fjording, M.; Bramm, E.; Binderup, L. Activities of the p38 MAP kinase inhibitor, EO1428, in three animal models of dermatitis. Fifth World Conference on Inflammation; Edinburgh, Scotland, September 22–26, 2001; Abstract 080.

(41) Amide derivatives useful for the treatment of diseases mediated by cytokines. *Exp. Opin. Ther. Pat.* **2001**, *11*, 1471–1473.

(42) Dumas, J.; Hatoum-Mokdad, H.; Sibley, R.; Riedl, B.; Scott, W. J.; Monahan, M. K.; Lowinger, T. B.; Brennan, C.; Natero, R.; Turner, T.; Johnson, J. S.; Schoenleber, R.; Bhargava, A.; Wilheim, S. M.; Housley, T. J.; Ranges, G. E.; Shrikhande, A. 1-Phenyl-5-pyrazolyl ureas: Potent and selective p38 kinase inhibitors. *Bioorg. Med. Chem. Lett.* **2000**, *10*, 2051–2054.

(43) Dumas, J.; Sibley, R.; Riedl, B.; Monahan, M. K.; Lee, W.; Lowinger, T. B.; Redman, A. M.; Johnson, J. S.; Kingery-Wood, J.; Scott, W. J.; Smith, R. A.; Bobko, R.; Schoenleber, R.; Ranges, G. E.; Housley, T. J.; Bhargava, A.; Wilheim, S. M.; Shrikhande, A. Discovery of a new class of p38 kinase inhibitors. *Bioorg. Med. Chem. Lett.* **2000**, *10*, 2047–2050.

(44) Redman, A. M.; Johnson, J. S.; Dally, R.; Swartz, S.; Wild, H.; Paulsen, H.; Caringal, Y.; Gunn, D.; Reneck, J.; Osterhout, M.; Kingery-Wood, J.; Smith, R. A.; Dumas, J.; Wilheim, S. M.; Housley, T. J.; Bhargava, A.; Ranges, G. E.; Shrikhande, A.; Young, D.; Bombara, M.; Scott, W. J. p38 Kinase inhibitors for the treatment of arthritis and osteoporosis: Thienyl, furyl and pyrrolyl ureas. *Bioorg. Med. Chem. Lett.* **2001**, *11*, 9–12.

(45) Pargellis, C. A.; Tong, L.; Churchill, L.; Cirillo, P.; Gilmore, T.; Graham, A. G.; Grob, P. M.; Hickey, E. R.; Moss, N.; Pav, S.; Regan, J. Inhibition of p38 map kinase by utilizing a novel allosteric binding site. *Nat. Struct. Biol.* **2002**, *9*, 268–272.

(46) Demers, J. P.; Klaubert, D. H. Addition of arylmetallics to azodicarboxylates: a novel synthesis of arylhydrazines by aromatic hydrazination. *Tetrahedron Lett.* **1987**, *28*, 4933–4934.

(47) Rosini, G.; Medici, A.; Soverini, M. Stereoselective, mild reduction of tosylhydazones with sodium cyanoborohydride in acidic media. *Synthesis* **1979**, 789.

(48) Krauss, J. C.; Cupps, T. L.; Wise, D. S.; Townsend, L. B. An efficient one-step synthesis of 3-oxoalkanenitriles. *Synthesis* **1983**, 308−309.

(49) Hackler, R. E.; Burow, K. W.; Kaster, S. V.; Wickiser, D. I. The synthesis of 5-amino-3-*tert*-butylisothiazole and 3-amino-5-*tert*-butylisothiazole. *J. Heterocycl. Chem.* **1989**, *26*, 1575−1578.

(50) Norwick, J. S.; Holmes, D. L.; Noronha, G.; Smith, E. M.; Nguyen, T. M.; Huang, S.-L. Synthesis of peptide isocyanates and isothiocyanates. *J. Org. Chem.* **1996**, *61*, 3929−3934.

(51) Krishnamurthy, S. A highly efficient and general N-monomethylation of functionalized primary amines via formylation−borane: dimethyl sulfide reduction. *Tetrahedron Lett.* **1982**, *23*, 3315−3318.

(52) Tong, L.; Pav, S.; White, D. M.; Rogers, S.; Crane, K. M.; Cywin, C. L.; Brown, M. L. A highly specific inhibitor of human p38 MAP kinase binds in the ATP pocket. *Nat. Struct. Biol.* **1997**, *4*, 311−316.

(53) Gallagher, T. F.; Fler-Thompson, S. M.; Garigipati, R. S.; Sorenson, M. E; Smietana, J. M.; Lee, D.; Bender, P. E.; Lee, J. C.; Laydon, J. T.; Griswold, D. E.; Chabot-Fletcher, M. C.; Breton, J. J.; Adams, J. L. 2,4,5-Triarylimidazole inhibitors of IL-1 biosynthesis. *Bioorg. Med. Chem. Lett.* **1995**, *5*, 1171−1176.

(54) The ^{1}H NMR of the ethoxy chain of **45** in DMSO indicates that populations of the gauche and staggered conformations are present. This information suggests that access to the gauche conformation needed for protein binding is not a high energy barrier. (Jones, P. Unpublished data).

(55) Wolfe, S. The gauche effect. Some stereochemical consequences of adjacent electron pairs and polar bonds. *Acc. Chem. Res.* **1972**, *5*, 102−111.

(56) Further pharmacological results will be reported shortly by J. Madwed and G. Nabozny.

(57) Branger, J.; van den Blink, B.; Weijer, S.; Madwed, J.; Bos, C. L.; Gupta, A.; Polmar, S. H.; Olszyna, D. P.; Hack, C. E.; van Deventer, S. J. H.; Peppelenbosch, M. P.; van der Poll, T. Antiinflammatory effects of a p38 mitogen activated protein kinase inhibitor during human endotoxemia. *J. Immunol.* **2002**, *168*, 4070−4077.

(58) Radziszewski, J. G.; Kaszynski, P.; Littmann, D.; Balaji, V.; Hess, B. A.; Michl, J. Twisted Si=N bonds: Matrix isolation of bridgehead silanimines. *J. Am. Chem. Soc.* **1993**, *115*, 8401−8408.

(59) Pav, S.; White, D. M.; Rogers, S.; Crane, K. M.; Cywin, C. L.; Davidson, W.; Hopkins, J.; Brown, M. L.; Pargellis, C. A.; Tong, L. Crystallization and preliminary crystallographic analysis of recombinant human p38 MAP kinase. *Protein Sci.* **1997**, *6*, 242−245.